

Supplementary Information

Table of contents

- Cluster annotations and pathway analyses
- Combined object and immune cells across CSF and blood compartments
- IL15 regulates immune responses in chronic active MS
- References
- Supplementary Figures

Cluster annotations and pathway analyses

CSF cells

L1 annotations of the CSF cells involved manual and Azimuth-based annotations. Subclustering was performed on the myeloid, T-cell and NK-related, and B-cell lineages (enclosed by dashed green, pink and blue lines) to obtain L2 cluster populations (Extended Figure 1A, C and Figure S5A-D).

T-cell and NK-related lineages: Among the T-cells, CD4 subsets were annotated as CD4⁺ Naïve, CD4⁺ Central Memory T (CD4 TCM), CD4⁺ Effector Memory (CD4 TEM) and CD4⁺ T-cells with Cytotoxic activity (CD4 CTL). Cluster defining genes for CD4 Naïve cells included *CCR7* (responsible for homing of T-cells to lymphoid organs), *FHIT*, and *NOG*¹. CD4 TCM and CD4 TEM both expressed *INPP4B*, *AQP3*, *FLT3LG*, *MAL*, and *CD40LG*, with CD4 TEM additionally expressing *GZMK*, *IFNG-AS1*, *LYAR*, and *DPP4* as the cluster-defining genes. CD4 CTL expressed *GZMH*, *NKG7*, and *LYAR*². CD8⁺ cells were marked by *CD8A*, *CD8B* which serve as co-receptors for the TCR³, and *KLRK1*, which encodes a cell-surface receptor expressed on activated CD8⁺ T cells⁴. *GZMH*, *GZMK*, *NKG7*, *CTSW*, and *CST7* genes differentiated CD8 TEM from CD8 TCM, reflecting the cytotoxic effector profile of CD8 TEM cells^{5,6}. *NELL2*, with its role in CD8⁺ T-cell differentiation, was a marker of CD8 Naïve and CD8 TCM cells⁷ but was also expressed by dnT cells. CD8⁺ proliferating cells, albeit a small cluster of cells, were marked by *CDT1*, *CLSPN*, *GINS2*, *UHRF1*, and *DTL* genes, which are involved in cell cycle regulation and epigenetic modifications⁸. Similarly, a CD4⁺ proliferating cell cluster comprised a small number of cells and was marked by *TYMS*, *RRM2*, *TK1*, *PCLAF*, and *UBEC2*, which are associated with cell proliferation and DNA synthesis and repair⁸.

dnT cell markers included *INPP4B*, *IFNG-AS1*, *GZMK*, and *TOX*, suggestive of cytotoxic functions, consistent with prior reports⁹. Note, *IFNG-AS1* is a long noncoding RNA (lncRNA) that acts as an enhancer for IFN- γ transcription and regulates its production at both transcriptional and translational levels¹⁰⁻¹². gdT ($\gamma\delta$ T-cells) were characterized by *TRDC*, *TRGV*, and *TRDV2* genes, which is expected since these are the TCR delta and gamma genes¹³. Mucosal-associated invariant T (MAIT) cells were identifiable using canonical markers, including *SLC4A10* (bicarbonate transporter with potential roles in maintaining pH and ion homeostasis for MAIT cells) and *TRAV1-2*, which is a TCR α -chain variable chain strongly associated with MAIT cells^{14,15}.

Top markers for innate lymphoid cells (ILC) included *TRDC*, *SPINK2*, *KIT*, *XCL1*, and *XCL2* genes. *XCL1* and *XCL2* as chemotactic cytokines have been shown previously to be markers of ILC, including natural killer (NK) cells¹⁶. NK

and NK_CD56bright cells differentially expressed the canonical markers including *KLRD1*, *KLRC1*, *KLRK1*, *GNLY*, *XCL1*, *XCL2*, *NKG7*, *TRDC*, and *CTSW*, discriminating these cells from the rest¹⁷. Regulatory T cells (Treg) exhibited the characteristic markers *FOXP3*, *TIGIT*, *IKZF2*, *RTKN2*^{18,19}; interestingly, we had a non-coding RNA (ncRNA), *AL136456.1*, as a Treg discriminatory marker as well.

Myeloid cells: L1 CSF myeloid cells were annotated as CD14 Mono, Mono1, Mono2, cDC2, cDC1, ASDC, and pDC. “CD14 Mono” cluster exhibited canonical markers such as *LYZ*, *FCN1*, *S100A9*, *S100A8*, and *VCAN*, suggestive of responses to Toll-like receptor (TLR) signaling, regulation of inflammatory processes, and cell adhesion/migration. Conventional dendritic cells type 2 (cDC2) showed expression of *FCER1A* (α -subunit of the high-affinity IgE receptor - Fc ϵ RI), *HLA-DQA1*, *CST3*, *CD1C*, and *HLA-DQB1* genes, representing of major histocompatibility complex (MHC) class II molecules and lipid antigen presentation^{20,21}. Previously defined markers, *XCR1* and *IRF8*, involved in cross-presentation of antigens to CD8 $^+$ T cells, development of cDC1 (conventional dendritic cells type 1), and antiviral responses, including regulation of IFN-stimulated genes (ISG), were found as discriminatory markers of cDC1 from cDC2 in our dataset^{22,23} – although we had additional discriminatory markers (*LGALS2*, *DNASE1L3*, *IDO1* and *TACSTD2*) as well. *TCF4* as one of the master regulator transcription factors (TF) for plasmacytoid dendritic cells (pDC) was found to be expressed in our dataset. In addition, *RHEX*, *CLEC4C*, and *LILRA4* were also expressed by pDC²¹. Presence of *SIGLEC6* and *PPP1R14A* differentiated AXL $^+$ *SIGLEC6 $^+$* dendritic cells (ASDC) from pDC²¹ in our dataset.

The cluster annotated as “Mono1” was marked by *C1QC*, *C1QA*, *C1QB*, *TYROBP*, *HLA-DRA*, *AIF1*, and *FCER1G* genes, while absent to decreased levels of expression of *LYZ*, *HLA-DQA1*, *HLA-DQB1*, and *MEF2C* in “Mono2” parsed the latter from the Mono1 cluster (Extended Figure 1C, Figure S5B). We performed unsupervised subclustering on all myeloid cell populations to obtain L2 clusters (Figure S6), with the overall interpretation of the subclusters and the pathway analyses provided below (see Methods — top 30 cluster defining genes were used):

- CD14M cluster showed enrichment of genes like *FCN1*, *VCAN*, *S100A8*, *S100A9*, *LGALS3*, *DYPD*, and *MTND2*. These genes represent terms like leukocyte aggregation, granulocyte chemotaxis, and positive regulation of inflammatory and defense responses (Figure S6B, C).
- M1 cluster showed association with genes responsible for regulation of K $^+$ ion transmembrane transport and monoatomic cationic homeostasis (*HAMP*, *SEL1L2*, *SLC12A5*, and *AL031056.1*).
- M2 was characterized by *TREM2*, *C3*, *A2M*, *SPP1*, *LIPA*, and *FOLR2* as the top marker genes, which represented terms such as regulation of receptor-mediated endocytosis (*C3*, *APOC1*, *APOC2*), synapse pruning (*C3*, *TREM2*), positive regulation of leukocyte chemotaxis (*CSF1R*, *CXCL12*, *CALR*), and regulation of lipid metabolic process (*APOC2*, *APOC1*, and *TREM2*). Notably, M3 expressed some of the same genes as M2, but the differentiating genes included *RHOB*, *TNFRSF1B*, *C5AR1*, *KLF2*, *JUNB*, *CEBPD*, and *ZFP36*. Pathway analyses for M3 showed response to lipopolysaccharide/LPS (*ZFP36*, *SLC11A1*, *CD14*, *TNFRSF1B*), phagocytosis and endocytosis (*MSR1*, *SLC11A1*, *CD14*, *CXCL16*) and inflammatory response (*CSF1R*, *SLC11A1*, *C5AR1*, *CD14*). The transcriptional profile of M3 bears some resemblance to previously described ‘microglia-like’ cells in the CSF²⁴ and to microglial phenotypes previously described in various neurodegenerative disorders²⁵⁻²⁷.
- M4 cluster enriched for markers like *IL32*, *CD3E*, *IL7R*, *CCL5*, *SKAP1*, and *CD247*, responsible for antigen receptor-mediated signaling (*ITK*, *LCK*, *CD247*, *SKAP1*) and T-cell activation (*CD2*, *ITK*, *LCK*, *CD247*).

- Cluster M5 had *PLXDC2*, *MT-ND1*, *NEAT1*, *LRMDA*, *SLC8A1*, *ARHGAP15*, *ZBTB20*, *FOXP2*, *SSH2*, and *ELMO1* as the cluster-defining genes. The pathways enriched included sodium ion transport across plasma membrane (*SLC9A9*, *SLC8A1*), myeloid leukocyte differentiation (*GAB2*, *FOXP1*), and regulation of small GTPase-mediated signal transduction (*STARD13*, *ARHGAP15*, *ARHGAP26*), among others. Note, comparison of cluster M5 to the immune cells from a previously published MRI-informed snRNAseq study showed that the clusters M3 and M5 were transcriptionally most like the microglia inflamed in MS (MIMS) phenotypes (MIMS-iron and MIMS-foamy) found at the CAL edge (Figure 2C)²⁸. In addition, M5 cluster transcriptionally bore resemblance to the microglia isolated from human Alzheimer's disease (AD) brains (Extended Figure 3C)²⁹.
- Cluster M6 likely represents “cycling myeloid cells,” enriched in terms like microtubule cytoskeleton organization involved in mitosis (*STMN1*, *PLK1*, *NUSAP1*, *CDK1*, *BIRC5*, *AURKB*, *SPC25*), mitotic cell cycle phase transition (*CCNA2*, *CCNB2*, *UBEC2*, *PLK1*, *CDK1*, *PKMYT1*, *CDKN3*), mitotic spindle organization (*TPX2*, *STMN1*, *PLK1*, *BIRC5*, *AURKB*, *SPC25*) and cell cycle G2/M phase transition (*CCNA2*, *PLK1*, *CDK1*, *PKMYT1*, *AURKB*), among others. The cluster-defining genes included *STMN1*, *TYMS*, *PCLAF*, *UBEC2*, *CDK1*, *NUSAP1*, *TK1*, *RMM2*, *TOP2A*, and *CDKN3*.
- M7 was marked by *ISG15*, *IFIT1*, *IFIT3*, *MX1*, *CXCL10*, *IFI4L*, *STAT1*, *GBP1*, *OAS3*, and *CMPK2* genes, and enriched in pathways including defense to virus/symbiont (*IFITM1*, *STAT1*, *MX2*, *MX1*, *IFI6*, *ISG15*, *IFIT1*, *USP18*, *IFIT3*, *IFI44L*, *IFIT2*, *OASL*, *CXCL10*, *OAS2*, *OAS3*), response to IFN- β (*IFITM1*, *PLSCR1*, *STAT1*, *XAF1*), and response to type-I IFN (*MX1*, *ISG15*, *USP18*).
- Cluster M8 was defined by terms including regulation of TLR-9 signaling and negative regulation of viral-induced cytoplasmic pattern recognition receptors (*PTPRS*, *LILRA4*), and differentiated from other clusters by *RHEX*, *BCL11A*, *UGCG*, *LILRA4*, *PLAC8*, *JCHAIN*, and *CLEC4C*. M9 was determined by presence of *CCL3*, *CCL4L2*, *IL1B*, *CCL4*, *EGR1*, *CCL3L1*, and *EGR2*. Pathway analyses showed enrichment for cellular response to interleukin-1/IL1 (*EGR1*, *CCL8*, *CCL3L1*, *IL1B*, *CCL4*, *CCL3*, *CCL2*), lymphocyte chemotaxis (*CH25H*, *CCL8*, *CCL3L1*, *CCL4*, *CCL3*, *CCL2*), regulation of ERK1 and ERK2 cascade/positive regulation of MAPK cascade (*PDGFRA*, *CCL8*, *CCL3L1*, *IL1B*, *CCL4*, *CCL3*, *CCL2*, *FGF10*), and response to IL1.
- M10 was defined by tryptophan metabolism (*IDO2*, *IDO1*) and BMP signaling pathway (*NOG*, *GDF7*).
- M11 was defined by *CCR7*, *LAMP3*, *BIRC3*, *CLLU1*, *LAD1*, *NOS1*, *NCCRP*, and *TFP12*, characterized by enrichment of processes like negative regulation of dendritic cell apoptosis, response to prostaglandin E, and nitric oxide (*CCR7*, *CCL19*).
- Cluster cDC2 enriched for regulation of leukocyte/T-cell mediated cytotoxicity (*CD1E*, *CD1C*), response to cytokines (*CIITA*, *FLT3*, *AFF3*), positive regulation of Ca^{2+} ion transmembrane transporter activity (*P2RY6*, *AP1B1*), C-type lectin receptors (*CLEC10A*), cytokine receptor activity (*FLT3*, *IL1R2*, *IL2RG*), and additional gene markers including *FCER1A*.
- Amongst the top genes discriminating cDC1 from cDC2 cluster included *XCR1*, *LGALS2*, and *IDO1*. Cluster cDC1 enriched for genes involved in regulation of mitotic nuclear division (*EPGN*, *RGCC*), tertiary granule and clathrin-coated endocytotic vesicle (*TCN1*, *EPGN*).

B-lymphoid lineage cells: Gene markers common to L1 annotations of B-naïve, Transitional-B and B-memory cells included *MS4A1*, *BANK1*, *CD79A*, and *RALGPS2*³⁰⁻³². Markers specific to B-naïve cells included *TCL1A* and *IGHM*, with *BLK* being discriminatory for B-memory cells versus other B-cell types. *AFF3* was expressed to a lesser extent by B-memory versus other clusters. Plasmablasts were enriched in *JCHAIN*, *MZB1*, *IGHA1*, *TXNDC5*, and *TNFRSF17*

genes³². For detailed characterization, subclustering was performed with the following clusters and functions (Figure S7):

- Cluster b1 is enriched in B-cell-receptor signaling and B-cell activation (*BLK*, *CD79B*, *MS4A1*, *BANK1*), response to cytokines (*SELL*, *CXCR4*, *AFF3*), regulation of signal transduction (*GNG7*, *CD24*, *CD55*), and positive regulation of T-cell proliferation (*TNFRSF13C*, *CD24*). The cluster-defining genes included *CXCR4*, *VPREB3*, *AFF3*, *TNFRSF13C*, *NIBAN3*, *TSC22D3*, *LINC00926*, *SNHG7*, and *SELL*.
- Cluster b2 was defined by expression of *IGKV1D-8*, *CD3E*, *IL7R*, *IGHV4-59*, *IL32*, *IGKV3-15*, *CST3*, *FYB1*, *GIMAP7*, *CD3G*, *INPP4B*, *IGHV4-61*, *IGKV3-11*, *GIMAP4*, *LINC00861*, *CD3D*, *HIST1H1E*, *MS4AGA*, and *KIF5C*. Pathways enriched for this cluster included T-cell activation, antigen-receptor mediated signaling pathway, and positive regulation of IL4 and FcεR-signaling pathway. Transcriptionally, cluster b2 most resembles the cells labeled as Plasmablast in L1 annotation (Figure S9E). Note, cluster b2 is also marked by *IL7R*, which has been shown to be expressed in early stages of B-cell lineage development^{33,34}. Interestingly, this cluster also showed expression of CD3-pertinent genes, which may be suggestive of a bi-phenotypic lymphocytic subset displaying both T- and B-cell functions³⁵, considering prior reports of the presence of CD20+ T cells in the CSF and blood of MS patients³⁶, and the aberrant presence of T-cell-associated antigens in B-cell lymphomas^{35,37}, or vice versa³⁸. This cluster also showed expression of immunoglobulin genes (Figure S7B), suggestive of B-cell function. The presence of canonical T-cell transcripts in b2 cluster could also be a possible result of prolonged contact between T and b2 cells. A prior study also reported CD3-positive B cells being a consequence of ex vivo storage of PBMC samples³⁹; however, it is pertinent to note that all the samples used (CSF and PBMC) were fresh in our study.
- Cluster b3 enriched for markers like *SOX5*, *ACP5*, *TNFRSF13B*, *ANXA4*, *CXCR3*, *FGR*, *ADGRG5*, *HMOX1*, and *RGCC* (Figure S7B). The terms associated with b3 cluster included positive regulation of cytokine production (*CD86*, *PYCARD*, *FGR*, *RGCC*, *SYK*, *HMOX1*, *POU2F2*), regulation of phagocytosis (*PYCARD*, *FGR*, *HCK*, *SYK*), Fcγ-receptor signaling pathway (*FGR*, *HCK*, *SYK*), and B-cell homeostasis (*TNFRSF13B*, *GAPT*)^{40,41}.
- Cluster b4 was characterized by mediation of the endoplasmic reticulum (ER)-associated degradation (ERAD) pathway (*XBP1*, *HSPA5*, *SELENOS*, *DERL3*, *MAN1A1*), response to ER stress (*XBP1*, *HSPA5*, *SELENOS*, *CREB3L2*, *PDIA4*), ubiquitin-dependent ERAD pathway, and negative regulation of apoptotic process (*MYDGF*, *XBP1*, *HSPA5*, *CD38*, *IGF1*, *TXNDC5*)⁴²⁻⁴⁴. Since ERAD pathway is critical for transitioning of large pre-B cells to small pre-B cells, it could be possible that these cells represent a lineage transition toward small pre-B cells, subsequently into immature B and/or mature B cells.
- Cluster b5 represented B-cell activation and differentiation (*PRKCB*, *PTPRJ*, *PAX5*, *HDAC9*), regulation of interleukin-2 (IL2) production (*HDAC9*, *CARD11*, *RUNX1*), regulation of B-cell receptor signaling (*PRKCB*, *FCRL3*), and negative regulation of Na⁺ transmembrane transporter activity (*CAMK2D*, *PRKCE*)^{45,46}. Significant cluster-defining markers included *PRKCB*, *PTPRJ*, *PAX5*, *HDAC9*, *CAMK2D*, *PRKCE*, *FCRL3*, *EIF4G3*, *SLC9A7*, and *SIPA1L3*^{30,33}.
- Cluster b6 — a very small cluster — enriched for *LAMP3*, *FSCN1*, *TPFPI2*, and *MGLL*. It showed terms like monocyte chemotaxis and response to tumor necrosis factor/TNF (*CCL22*, *TNFRSF11A*, *CCL19*) and tryptophan metabolic process (*IL4I1*, *IDO1*).

PBMC

L1 annotations of the PBMC were performed using a reference dataset⁴⁷. Subclustering was performed on the myeloid, T-cell and NK-related, and B-cell lineages to obtain L2 cluster populations (Extended Figure 1B, D and Figure S5E-H). Most of the L1 cluster-defining genes for the PBMC were the same as L1 CSF cluster-defining genes, particularly in the T-cell and NK-related lineages and B-lymphoid lineages, unless otherwise stated.

T-cell and NK-related lineages: For PBMC in the periphery, cluster-defining genes for CD4 Naïve were the same as for CSF: *CCR7* and *FHIT*¹, but also *LEF1* and *TCF7* (encodes TCF1 – a key transcription factor in T-cell development and differentiation)^{48,49}. For CD8 Naïve cells, the cluster-defining genes were similar with the addition of *CD8A* and *CD8B*. CD4 TCM and CD4 TEM were both defined by expression of the canonical marker *IL7R*³⁴, but CD4 TEM expressed *GZMK* while CD4 TCM *INPP4B* and *MAL*. CD4 CTL expressed similar markers as CSF but had additionally the expression of *CCL5*². CD8 TEM was differentiated from CD8 TCM by expression of *GZMH*, *NKG7*, *GNLY*, *GZMA*, *CCL5/RANTES* in the effector memory phenotype, suggestive of a cytotoxic profile like that seen in the CSF^{5,6}. dnT was characterized by expression of *IFNG-AS1* and *GZMK*. $\gamma\delta$ T expressed TCR-delta and gamma genes, in addition to *DUSP2*. MAIT were identifiable by *KLRB1*, *SLC4A10*, and *DUSP2*^{14,15,50}. NK and NK_CD56bright expressed the same canonical genes (*KLRD1*, *GZMH*, *GNLY*, *NKG7*) as described above for CSF, with *XCL1* and *XCL2* discriminating latter from the prior in the blood⁴⁹. Treg were identifiable using essentially the same markers in the periphery as the CSF.

Myeloid lineage cells: L1 annotations of myeloid lineage cells in the blood included CD14 Mono, CD16 Mono, cDC1, cDC2, ASDC, and pDC. Note, we have been characterizing pDC as part of myeloid lineage cells despite there being evidence of pDC being derived from common lymphoid progenitors in addition to myeloid-based lineage, based on the clustering^{51–54}. cDC2 and cDC1 were identifiable by the canonical expression of genes like *HLA-DQA1*, *HLA-DQB1*, *HLA-DRB5*, and *CPVL*^{20,21,55}, with *FCER1A*, *S100A9*, and *VCAN* expression in cDC2 parsing it from cDC1. cDC1 cells were characterized by the expression of *CLEC9A*, *IDO1*, *DNASE1L3* and *XCR1*. CD14 Mono was defined by *S100A8*, *S100A9*, *VCAN*, and *FCN1* expression which is identical to CSF, while CD16 Mono cells were characterized by the expression of *FCGR3A* (*CD16/Fc γ RIII*; also expressed by NK), *MS4A7*, *SMIM25*, *SERPINA1*, and *TCF7L2*²¹. ASDC in the periphery expressed the same markers as in the CSF (Figure S5B, F). pDC were identifiable using *TCF4*, *PLD4*, *CCDC50*, *JCHAIN*, *LILRA4*, *IL3RA* (*CD123*), *CLEC4A*, and *SERPINF1* expression^{52–54}.

We subclustered the above-mentioned myeloid cells for better understanding of cell phenotypes (Figure S8A-C). The following are the subclusters defined:

- CD14M_1 was characterized by negative regulation of peptidase/endopeptidase activity (*SERPINB10*, *SERPINB2*, *SERPINI2*, *NRG1*) and lipid oxidation (*ALOX15B*, *PLA2G7*) while CD14M_2 enriched for vitamin transport, water-soluble vitamin metabolic process (*SLC2A3*, *FOLR3*, *VNN2*), and organic anion transport (*ABCC6*, *SLC2A3*).
- CD14M_2 was discriminated from CD14M_1 by expression of genes involved in detoxification processes, lipid hydrolysis, and citrullination for NETosis in neutrophils (*MGST1*, *CES1*, *PADI4*)^{56–58}, clearance of apoptotic cells (*STAB1*)⁵⁹, and phospholipid metabolism (*PLA2G7*), among others.

- CD14M_3 showed gene expression significant for antigen presentation of peptide antigen via MHC class II (*HLA-DMB*, *HLA-DOA*, *HLA-DQA2*, *HLA-DQA1*) and positive regulation of leukocyte chemotaxis (*CSF1R*, *CALR*). The cluster defining genes included *HLA-DQA1*, *CSF1R*, *MARCKS*, *CALR*, and *LIPA*^{21,60}.
- CD14M_4 cluster enriched for defense responses against symbiont/virus or negative regulation of viral processes, IL-27 signaling, antiviral innate immune response, positive regulation of type-I IFN production, IFN- α / β signaling, ISG15 antiviral mechanism, and IFN- γ signaling (*STAT1*, *STAT2*, *MX1*, *MX2*, *IFI6*, *EIF2AK2*, *ISG15*, *IFIT1*, *IFI44L*, *IFIT3*, *IFIT2*, *OASL*, *OAS2*, *OAS3*, *IRF7*, *RSAD2*, *HERC*, *OASL*)^{61,62}.
- CD14M_5 was defined by inflammatory response (*CXCL8*, *CCL3L1*, *TNFAIP6*, *IRAK2*, *RIPK2*, *IL1B*, *CCL4*, *CCL3*, *NLRP3*, *CXCL2*), cellular response to IL-1 (*EGR1*, *CXCL8*, *CCL3L1*, *IRAK2*, *IL1B*, *CCL4*, *CCL3*), cellular response to LPS, granulocyte migration, chemokine activity (*CXCL8*, *CCL3L1*, *CCL4*, *CCL3*, *CXCL2*), and NF κ B signaling (*CXCL8*, *CCL4L2*, *IL1B*, *CCL4*, *TNFAIP3*, *PTGS2*, *CXCL2*, *ICAM1*).
- CD14M_6 cluster was enriched in activation of GTPase activity (*TBC1D5*, *TBC1D22A*, *ARHGAP24*), positive regulation of protein tyrosine kinase activity (*FBXW7*, *NEDD9*), regulation of glycolytic process (*PKRAG2*), positive regulation of myeloid leukocyte differentiation and biosynthetic processes (*NEDD9*, *RUNX1*, *ZBTB20*). This is suggestive of cytoskeletal dynamics, cell differentiation and proliferation, and immune activation⁶³.
- CD14M_7 was defined by chemokine-mediated signaling (*CCL5*, *PPBP*, *PF4V1*, *PF4*), myeloid cell and megakaryocyte development (*GP9*, *MPIG6B*, *GP1BB*), and negative regulation of Ca $^{2+}$ sequestering (*CLU*, *GP1BB*).
- CD14M_8 enriched for a multitude of lncRNAs (Figure S8B), including *VCAN-AS1*, *CPB2-AS1*, and *DPYD-AS1*, suggesting that this cluster may have regulatory roles in gene expression and additional processes.
- CD16M_1 cluster was characterized by positive regulation of actin filament bundle assembly, cellular response to fluid shear stress, cell-cell junction maintenance (*EVL*, *RHOC*, *MTSS1*, *KLF2*, *CSF1R*), negative regulation of cell population proliferation, and apoptosis (*CDKN1C*, *IFITM1*, *HMOX1*, *MTSS1*, *TCF7L2*).
- CD16M_2 showed enrichment of similar terms, including positive regulation of intracellular transduction (*CX3CR1*, *TCF7L2*, *PTP4A3*, *HMOX1*, *LTB*, *RHOC*).
- cDC represented similar MHC class-II protein class assembly and MHC-II restricted antigen presentation terms (*HLA-DOA*, *HLA-DQA2*, *HLA-DQA1*, *FCER1A*), progenitor cell differentiation (*FLT3*, *PLD4*), and antigen (including lipid) presentation (*CD1C*, *CD1E*), as described above²¹.
- pDC showed the same markers and functions as above.
- The “Mono” cluster showed antigen receptor-mediated signaling and T-cell activation (*ITK*, *TRBC2*, *CD247*, *CD3E*, *CD3D*, *SKAP1*), which could be a result of the myeloid cell cluster being in contact with adaptive immune cells or a clustering artifact.

B-lymphoid lineage cells: L1 annotations for B-lymphoid cells in the blood had the same markers as in CSF, including *MS4A1*, *BANK1*, *CD79A*, *RALGPS2*, and *BLK*³⁰⁻³². The following are the subclusters and pathway analyses performed (Figure S9A-D):

- Cluster b1 enriched in cellular response to cytokines (*IL4R*, *CCR7*, *YBX3*) and negative regulation of cytokine production (*APLP2*, *CD200*). This cluster may represent IgM $^{\text{low}}$ transitional B-cells³³.
- Cluster b2 was defined by B-cell receptor signaling pathway (*IGHG1*, *IGHG2*, *IGHA1*) and regulation of B cell proliferation and B-cell activation (*TNFRSF13B*, *GPR183*, *CD27*).

- Cluster b3 showed expression of genes involvement in negative regulation of inflammatory response (*FGR*, *HCK*, *GRN*, *TNFRSF1B*) and positive regulation of T-helper 1 type immune response (*SLC11A1*, *TBX21*).
- Cluster b4 is defined by positive regulation of cell-substrate adhesion (*CDK6*, *JUP*, *LIMS2*), regulation of B-cell proliferation, and B-cell-receptor signaling pathway (*MZB1*, *CD38*, *IGLC1*).
- Cluster b5 enriched in regulation of Na^+ ion transmembrane transporter activity (*CAMK2D*, *PRKCE*, *UTRN*), $\text{F}_c\gamma$ - and F_c -receptor signaling pathway in phagocytosis (*VAV3*, *PRKCE*), and actin cytoskeleton reorganization (*SIPA1L1*, *AUTS2*) and phosphorylation (*CAMK2D*, *PRKCE*, *SIK3*, *CDK14*).
- Cluster b6 represented terms including $\alpha\beta$ T-cell activation (*NKG7*, *CD247*, *CD3E*, *CD3D*), granulocyte chemotaxis (*ANXA1*, *CCL5*), and genes like *IL32*, *TYROBP*, and *GNLY*. This peripheral B-cell cluster was transcriptionally most similar to the b2 cluster in the CSF (Figure S9D), therefore, more likely to resemble plasmablast (see above for CSF b2 cluster). Other cluster markers are shown in Figure S9B.

Note that for both the CSF cells and PBMC, we projected the L2 annotations onto L1 space, supporting the sub-clustering scheme (Figure S5C-D, G-H).

Combined object and immune cells across CSF and blood compartments

Integrating the CSF and PBMC samples, we created a combined object (Figure S8B), with level 2 (L2) cell annotations mapped onto it (Figure S8C). In this combined object, the myeloid cells from CSF clustered separately from the myeloid cells of PBMC origin (Figure S8C, D). This is consistent with the diversity of CSF macrophages and the unique niche they occupy⁶⁴. Most of the overlap between CSF- and PBMC-derived myeloid cells occurred among dendritic cells across the two compartments.

The adaptive immune cells from both CSF and blood, on the other hand, clustered together. However, in the non-perturbed samples (untreated and radiologically inactive PRL-positive vs. PRL-negative) and across the compartments, CD8-TEM and CD4-TCM cells upregulated genes associated with integrin signaling and migration (*CXCR3*, *CXCR4*, *CXCR6*, *CCL5*, *ITGA4*) and cytotoxicity (*GZMK*, *GZMA*) in CSF relative to blood (Figure S8E, F). This aligns with a recent report describing upregulation of genes associated with migration in CD8⁺ and CD4⁺ T cells in the CSF relative to PBMC⁶⁵.

The NK cells in the CSF were enriched in pathways pertinent to eukaryotic translation and lymphotoxin receptor signaling relative to blood (Figure S8F). Notably, *GZMK* was one of the most enriched genes in CD8-TEM cells from CSF relative to blood (Figure S8E). Since we find clonal expansion of CD8-TEM cells in PRL-positive vs. PRL-negative cases in both blood and CSF, this suggests that clonally expanded CD8-TEM cells may acquire an even more cytotoxic signature upon trafficking from the blood to the CSF, consistent with their relevance to mediation of chronic neuroinflammation in PRL-positive cases.

IL15 regulates immune responses in chronic active MS

To determine how the immune environment might be modulating the transcriptomic changes across cells from PRL-positive versus PRL-negative cases in both blood and CSF, we performed NicheNet analyses, which interrogate

predicted ligand-receptor interactions. We found *IL15* and *TNFSF12* (TWEAK) to be the predicted regulatory ligands of the target genes for myeloid (Figure S9A) cells in blood. This is consistent with prior reports implicating IL15-induced pro-inflammatory responses in MS and experimental autoimmune encephalomyelitis (EAE)^{66,67}. Previously, TWEAK+ cells were found to be frequent at the edges of chronic active lesion edges and in subpial cortical lesions, suggesting a potential role of TNFSF12-mediated signaling in such lesions⁶⁸. We also found *TNFSF10* (TRAIL) to be modulating the transcriptional changes in blood myeloid cells in the PRL-positive state.

Interestingly, *CD40*, expressed by B cells, was predicted to be a critical regulator of the transcriptional changes in CD4 T-cells in blood (Figure S9B), whereas *CD40LG* was a predicted regulatory ligand for myeloid cells. CD40-CD40LG costimulatory signaling is critical in regulating the initiation of adaptive and innate immune cellular processes, with recent approaches involving the therapeutic targeting of *CD40LG* with a monoclonal antibody in MS^{69,70}. For NK cells, *LTB*, *CD40LG*, and *APP* were among the top regulatory ligands driving the differentially expressed genes across PRL-positive versus PRL-negative cells (Figure S9C). In the case of *LTB*, its interaction with *LT β R* on NK-cell induces innate immune responses⁷¹. For CD8 T-cells, *CD48*, *GRN*, and *SECTM1* were among the main predicted regulatory ligands, with the latter acting as a co-stimulatory ligand to stimulate CD8 T-cell proliferation and cytokine production⁷² (Figure S9D). For B-cells, predicted regulatory ligands included *LGALS3BP* and HLA molecules (Figure S9E).

In terms of the prioritized differential ligand-receptor interactions in blood, we found HLA-I molecules on NK cells to be interacting with various receptors, including *LILRB1* and *ITGB2*, on myeloid cells; *KLRK1*, *KLRC2* and *KIR3DL1* on NK cells; and *CD8A* and *KLRK1* on CD8 T-cells (Figure S9F). These ligand-receptor interactions have an immuno-regulatory potential, with interactions involving *CD8A* and *KLRK1* receptors promoting T-cell activation and cytotoxicity, and *LILRB1* acting as inhibitory receptors for MHC-I class molecules, thereby dampening myeloid-mediated immune responses⁷³. Similarly, galectins (*LGALS1* and *LGALS9*) on myeloid cells interacted with *PTPRC* on NK cells, and they have been shown to modulate immune responses⁷⁴.

In the CSF, the top predicted molecules regulating the target genes in PRL-positive cases included *TNF* from CD4 T-cells and *TGFB1* from NK cells (Figure S9G). In the CD8 $^+$ T-cells, *TNF* from CD4 T-cells emerged as the predicted molecule driving the differentially expressed genes across PRL-positive vs. PRL-negative cells (Figure S10A). The central target gene modulated by the predicted regulators in both myeloid and CD8 $^+$ T-cells of the CSF was *LTB*, which plays a role in tertiary lymphoid organization in leptomeninges⁷⁵. *B2M* and *COL9A2* from CD8 $^+$ T-cells and cDC, respectively, were the main predicted ligands for NK cells, while *TGFB1* and *CD40LG* were the predicted ligands for CD4 T-cells (Figure S10B, C). The prioritized ligand-receptor interactions in CSF were significant for myeloid *C3* and *APOE* as the ligands for *ITGB2* and *TREM2* receptors respectively on myeloid cells. *APOE-TREM2* interaction has been implicated in switching of the microglia to a neurodegenerative phenotype⁷⁶. Concordantly, our proteomic data showed abundance of TREM2 in the CSF of patients with a high burden of PRL (PRL \geq 4) vs. low burden (PRL 1-3; $p = 0.08$) and no-PRL ($p = 0.1$). In addition, we also found enrichment of *IL15* in the CSF of cases with high PRL burden relative to low PRL ($p = 0.003$) and no PRL ($p = 0.0007$) (Figure S10E).

References

1. Yasumizu, Y. et al. Single-cell transcriptome landscape of circulating CD4+ T cell populations in autoimmune diseases. *Cell Genomics* **4**, 100473 (2024).
2. Takeuchi, A. & Saito, T. CD4 CTL, a Cytotoxic Subset of CD4+ T Cells, Their Differentiation and Function. *Front Immunol* **8**, (2017).
3. Gao, G. F. & Jakobsen, B. K. Molecular interactions of coreceptor CD8 and MHC class I: the molecular basis for functional coordination with the T-cell receptor. *Immunol Today* **21**, 630–636 (2000).
4. Tsyklauri, O. et al. Regulatory T cells suppress the formation of potent KLRK1 and IL-7R expressing effector CD8 T cells by limiting IL-2. *Elife* **12**, (2023).
5. Wang, X.-M. et al. Global transcriptomic characterization of T cells in individuals with chronic HIV-1 infection. *Cell Discov* **8**, 29 (2022).
6. Zhang, J.-Y. et al. Single-cell landscape of immunological responses in patients with COVID-19. *Nat Immunol* **21**, 1107–1118 (2020).
7. Buggert, M. et al. The Identity of Human Tissue-Emigrant CD8+ T Cells. *Cell* **183**, 1946–1961.e15 (2020).
8. Altorki, N. K. et al. A signature of enhanced proliferation associated with response and survival to anti-PD-L1 therapy in early-stage non-small cell lung cancer. *Cell Rep Med* **5**, 101438 (2024).
9. Yang, L. et al. Transcriptome landscape of double negative T cells by single-cell RNA sequencing. *J Autoimmun* **121**, 102653 (2021).
10. Peng, H. et al. The Long Noncoding RNA IFNG-AS1 Promotes T Helper Type 1 Cells Response in Patients with Hashimoto’s Thyroiditis. *Sci Rep* **5**, 17702 (2015).
11. Ali, M. A. et al. The Ifng antisense RNA 1 (IFNG-AS1) and growth arrest-specific transcript 5 (GAS5) are novel diagnostic and prognostic markers involved in childhood ITP. *Front Mol Biosci* **9**, (2022).
12. Li, H. & Tsokos, G. C. Double-negative T cells in autoimmune diseases. *Curr Opin Rheumatol* **33**, 163–172 (2021).
13. Hu, Y. et al. $\gamma\delta$ T cells: origin and fate, subsets, diseases and immunotherapy. *Signal Transduct Target Ther* **8**, 434 (2023).
14. Shi, J. et al. Single-Cell Transcriptomic Profiling of MAIT Cells in Patients With COVID-19. *Front Immunol* **12**, (2021).
15. Godfrey, D. I., Koay, H.-F., McCluskey, J. & Gherardin, N. A. The biology and functional importance of MAIT cells. *Nat Immunol* **20**, 1110–1128 (2019).
16. Hashemi, E., McCarthy, C., Rao, S. & Malarkannan, S. Transcriptomic diversity of innate lymphoid cells in human lymph nodes compared to BM and spleen. *Commun Biol* **7**, 769 (2024).
17. Rebuffet, L. et al. High-dimensional single-cell analysis of human natural killer cell heterogeneity. *Nat Immunol* **25**, 1474–1488 (2024).
18. Luo, Y. et al. Single-cell transcriptomic analysis reveals disparate effector differentiation pathways in human Treg compartment. *Nat Commun* **12**, 3913 (2021).
19. Dikiy, S. & Rudensky, A. Y. Principles of regulatory T cell function. *Immunity* **56**, 240–255 (2023).

20. Hillman, H. *et al.* Single-cell profiling reveals distinct subsets of CD14+ monocytes drive blood immune signatures of active tuberculosis. *Front Immunol* **13**, (2023).
21. Villani, A.-C. *et al.* Single-cell RNA-seq reveals new types of human blood dendritic cells, monocytes, and progenitors. *Science* (1979) **356**, (2017).
22. Jirmo, A. C. *et al.* Single cell RNA sequencing reveals distinct clusters of Irf8-expressing pulmonary conventional dendritic cells. *Front Immunol* **14**, (2023).
23. Guilliams, M. *et al.* Unsupervised High-Dimensional Analysis Aligns Dendritic Cells across Tissues and Species. *Immunity* **45**, 669–684 (2016).
24. Farhadian, S. F. *et al.* Single-cell RNA sequencing reveals microglia-like cells in cerebrospinal fluid during virologically suppressed HIV. *JCI Insight* **3**, (2018).
25. Sankowski, R. *et al.* Mapping microglia states in the human brain through the integration of high-dimensional techniques. *Nat Neurosci* **22**, 2098–2110 (2019).
26. Keren-Shaul, H. *et al.* A Unique Microglia Type Associated with Restricting Development of Alzheimer’s Disease. *Cell* **169**, 1276–1290.e17 (2017).
27. Masuda, T. *et al.* Spatial and temporal heterogeneity of mouse and human microglia at single-cell resolution. *Nature* **566**, 388–392 (2019).
28. Absinta, M. *et al.* A lymphocyte–microglia–astrocyte axis in chronic active multiple sclerosis. *Nature* **597**, 709–714 (2021).
29. Prater, K. E. *et al.* Human microglia show unique transcriptional changes in Alzheimer’s disease. *Nat Aging* **3**, 894–907 (2023).
30. Verstegen, N. J. *et al.* Single-cell analysis reveals dynamics of human B cell differentiation and identifies novel B and antibody-secreting cell intermediates. *Elife* **12**, (2023).
31. Lee, R. D. *et al.* Single-cell analysis identifies dynamic gene expression networks that govern B cell development and transformation. *Nat Commun* **12**, 6843 (2021).
32. Morgan, D. & Tergaonkar, V. Unraveling B cell trajectories at single cell resolution. *Trends Immunol* **43**, 210–229 (2022).
33. Morgan, D. & Tergaonkar, V. Unraveling B cell trajectories at single cell resolution. *Trends Immunol* **43**, 210–229 (2022).
34. Mazzucchelli, R. & Durum, S. K. Interleukin-7 receptor expression: intelligent design. *Nat Rev Immunol* **7**, 144–154 (2007).
35. zhang, Y. *et al.* A biphenotypic lymphocyte subset displays both T- and B-cell functionalities. *Commun Biol* **7**, 28 (2024).
36. von Essen, M. R. *et al.* Proinflammatory CD20+ T cells in the pathogenesis of multiple sclerosis. *Brain* **142**, 120–132 (2019).
37. Pan, Z. *et al.* CD3-positive plasmablastic B-cell neoplasms: a diagnostic pitfall. *Modern Pathology* **31**, 718–731 (2018).
38. Tsuyama, N. *et al.* Clinical and prognostic significance of aberrant T-cell marker expression in 225 cases of *de novo* diffuse large B-cell lymphoma and 276 cases of other B-cell lymphomas. *Oncotarget* **8**, 33487–33500 (2017).
39. Nagel, A. *et al.* CD3-Positive B Cells: A Storage-Dependent Phenomenon. *PLoS One* **9**, e110138 (2014).
40. Takai, T. Roles of Fc receptors in autoimmunity. *Nat Rev Immunol* **2**, 580–592 (2002).
41. Martínez-Riaño, A. *et al.* Antigen phagocytosis by B cells is required for a potent humoral response. *EMBO Rep* **19**, (2018).

42. Jiang, Y., Tao, Z., Chen, H. & Xia, S. Endoplasmic Reticulum Quality Control in Immune Cells. *Front Cell Dev Biol* **9**, (2021).

43. Ji, Y. *et al.* The Sel1L-Hrd1 Endoplasmic Reticulum-Associated Degradation Complex Manages a Key Checkpoint in B Cell Development. *Cell Rep* **16**, 2630–2640 (2016).

44. Kong, S. *et al.* Endoplasmic reticulum-resident E3 ubiquitin ligase Hrd1 controls B-cell immunity through degradation of the death receptor CD95/Fas. *Proceedings of the National Academy of Sciences* **113**, 10394–10399 (2016).

45. Feher, A. *et al.* Functional Voltage-Gated Sodium Channels Are Present in the Human B Cell Membrane. *Cells* **11**, 1225 (2022).

46. Griss, J. *et al.* B cells sustain inflammation and predict response to immune checkpoint blockade in human melanoma. *Nat Commun* **10**, 4186 (2019).

47. Hao, Y. *et al.* Integrated analysis of multimodal single-cell data. *Cell* **184**, 3573–3587.e29 (2021).

48. Escobar, G., Mangani, D. & Anderson, A. C. T cell factor 1: A master regulator of the T cell response in disease. *Sci Immunol* **5**, (2020).

49. Terekhova, M. *et al.* Single-cell atlas of healthy human blood unveils age-related loss of NKG2C+GZMB-CD8+ memory T cells and accumulation of type 2 memory T cells. *Immunity* **56**, 2836–2854.e9 (2023).

50. Kovanen, P. E. *et al.* T-cell Development and Function Are Modulated by Dual Specificity Phosphatase DUSP5. *Journal of Biological Chemistry* **283**, 17362–17369 (2008).

51. Araujo, A. M. *et al.* Lymphoid origin of intrinsically activated plasmacytoid dendritic cells in mice. *Elife* **13**, (2024).

52. Swiecki, M. & Colonna, M. The multifaceted biology of plasmacytoid dendritic cells. *Nat Rev Immunol* **15**, 471–485 (2015).

53. Adams, N. M., Das, A., Yun, T. J. & Reizis, B. Ontogeny and Function of Plasmacytoid Dendritic Cells. *Annu Rev Immunol* **42**, 347–373 (2024).

54. Colonna, M., Trinchieri, G. & Liu, Y.-J. Plasmacytoid dendritic cells in immunity. *Nat Immunol* **5**, 1219–1226 (2004).

55. Harris, J. *et al.* A vitellogenin-like carboxypeptidase expressed by human macrophages is localized in endoplasmic reticulum and membrane ruffles. *Int J Exp Pathol* **87**, 29–39 (2006).

56. Siritantikorn, A. *et al.* Protection of cells from oxidative stress by microsomal glutathione transferase 1. *Biochem Biophys Res Commun* **355**, 592–596 (2007).

57. Tabas, I. & Bornfeldt, K. E. Macrophage Phenotype and Function in Different Stages of Atherosclerosis. *Circ Res* **118**, 653–667 (2016).

58. Ho, J. W., Quan, C., Gauger, M. A., Alam, H. B. & Li, Y. ROLE OF PEPTIDYLARGININE DEIMINASE AND NEUTROPHIL EXTRACELLULAR TRAPS IN INJURIES: FUTURE NOVEL DIAGNOSTICS AND THERAPEUTIC TARGETS. *Shock* **59**, 247–255 (2023).

59. Park, S.-Y. *et al.* Stabilin-1 mediates phosphatidylserine-dependent clearance of cell corpses in alternatively activated macrophages. *J Cell Sci* **122**, 3365–3373 (2009).

60. Stanley, E. R. & Chitu, V. CSF-1 Receptor Signaling in Myeloid Cells. *Cold Spring Harb Perspect Biol* **6**, a021857–a021857 (2014).

61. Ivashkiv, L. B. & Donlin, L. T. Regulation of type I interferon responses. *Nat Rev Immunol* **14**, 36–49 (2014).

62. Platanias, L. C. Mechanisms of type-I- and type-II-interferon-mediated signalling. *Nat Rev Immunol* **5**, 375–386 (2005).
63. O’Neill, L. A. J., Kishton, R. J. & Rathmell, J. A guide to immunometabolism for immunologists. *Nat Rev Immunol* **16**, 553–565 (2016).
64. Munro, D. A. D., Movahedi, K. & Priller, J. Macrophage compartmentalization in the brain and cerebrospinal fluid system. *Sci Immunol* **7**, (2022).
65. Mittl, K. *et al.* Antigen specificity of clonally-enriched CD8+ T cells in multiple sclerosis. Pre-print at <https://doi.org/10.1101/2024.09.07.611010> (2024).
66. Laurent, C. *et al.* Interleukin-15 enhances proinflammatory T-cell responses in patients with MS and EAE. *Neurol Neuroimmunol Neuroinflamm* **8**, (2021).
67. Rentzos, M. *et al.* IL-15 is elevated in serum and cerebrospinal fluid of patients with multiple sclerosis. *J Neurol Sci* **241**, 25–29 (2006).
68. Serafini, B. *et al.* Expression of TWEAK and Its Receptor Fn14 in the Multiple Sclerosis Brain: Implications for Inflammatory Tissue Injury. *J Neuropathol Exp Neurol* **67**, 1137–1148 (2008).
69. Vermersch, P. *et al.* Inhibition of CD40L with Frexalimab in Multiple Sclerosis. *New England Journal of Medicine* **390**, 589–600 (2024).
70. Elgueta, R. *et al.* Molecular mechanism and function of CD40/CD40L engagement in the immune system. *Immunol Rev* **229**, 152–172 (2009).
71. Tersteegen, A. *et al.* Lymphotoxin β Receptor: a Crucial Role in Innate and Adaptive Immune Responses against Toxoplasma gondii. *Infect Immun* **89**, (2021).
72. Wang, T. *et al.* K12/SECTM1, an interferon- γ regulated molecule, synergizes with CD28 to costimulate human T cell proliferation. *J Leukoc Biol* **91**, 449–459 (2011).
73. Barkal, A. A. *et al.* Engagement of MHC class I by the inhibitory receptor LILRB1 suppresses macrophages and is a target of cancer immunotherapy. *Nat Immunol* **19**, 76–84 (2018).
74. Liu, F.-T. & Stowell, S. R. The role of galectins in immunity and infection. *Nat Rev Immunol* **23**, 479–494 (2023).
75. Zuo, M., Wang, A. A. & Gommerman, J. L. Follicle on the Roof: Tertiary Lymphoid Structures in Central Nervous System Autoimmunity. *Immunol Rev* **332**, (2025).
76. Krasemann, S. *et al.* The TREM2-APOE Pathway Drives the Transcriptional Phenotype of Dysfunctional Microglia in Neurodegenerative Diseases. *Immunity* **47**, 566-581.e9 (2017).

Fig. S1

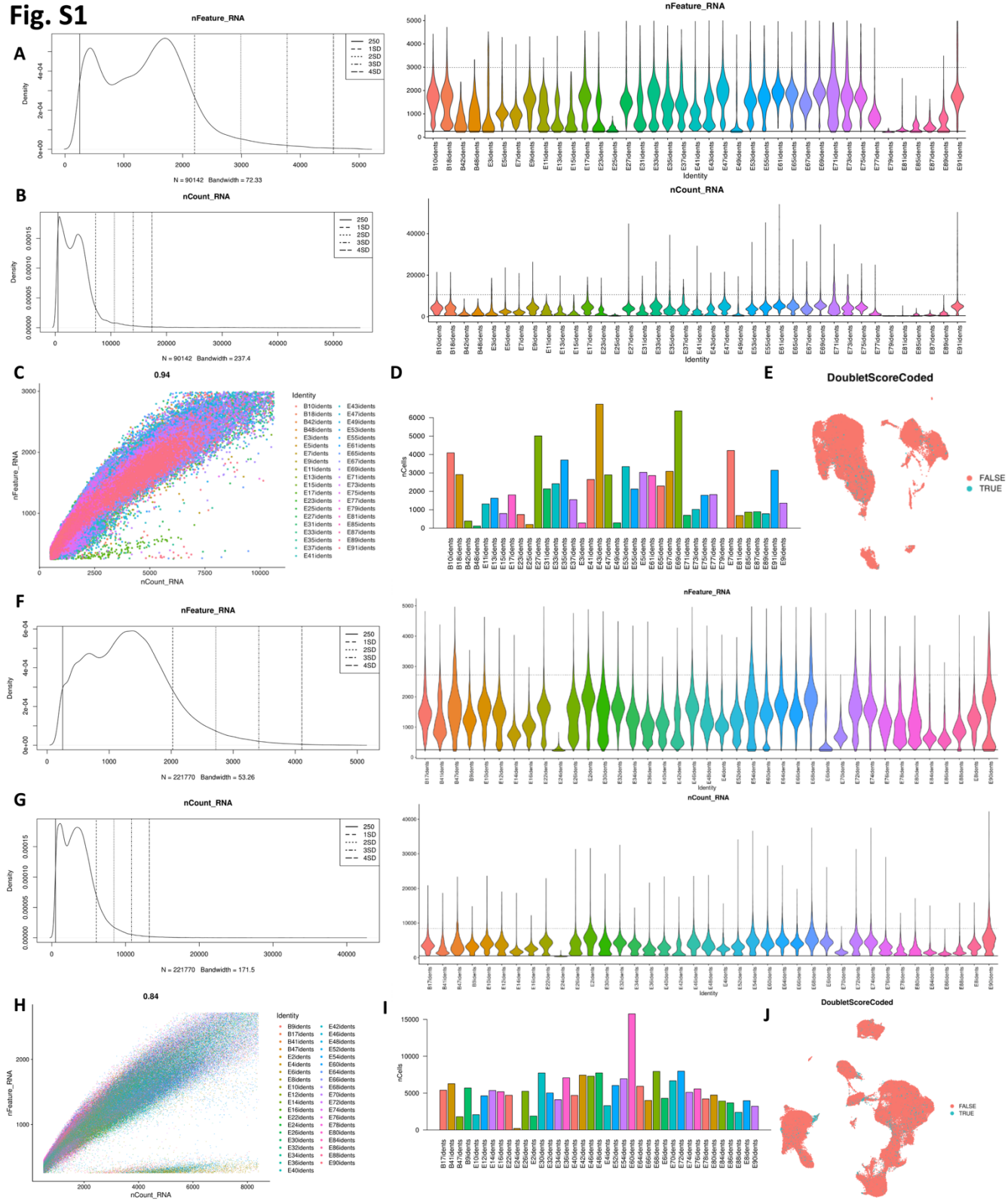
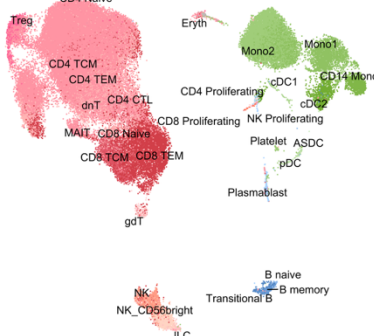


Figure S1: Quality control (QC) metrics for CSF and PBMC objects

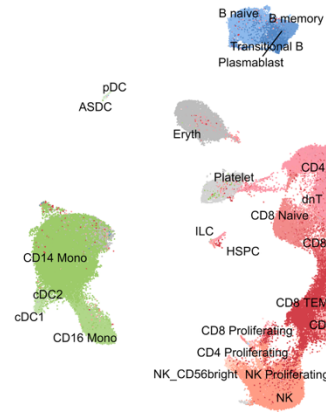
- a) Pre-filtering density curve for nFeature_RNA (left panel) — unique features (genes) — identified and violin plot (right panel) showing nFeature_RNA per CSF sample.
- b) Pre-filtering density curve for nCount_RNA (left panel) — total number of genes detected — and violin plot (right panel) demonstrating counts per CSF sample.
- c) Post-filtering scatter plot showing high correlation between nCount_RNA and nFeature_RNA for the CSF object.
- d) Post-filtering cell counts per CSF sample. E79 was excluded from further analyses.
- e) UMAP illustrating doublets that were excluded from analyses.
- f) Pre-filtering density curve for nFeature_RNA (left panel) and violin plot (right panel) showing nFeature_RNA per PBMC sample.
- g) Pre-filtering density curve for nCount_RNA (left panel) and violin plot (right panel) demonstrating counts per PBMC sample.
- h) Post-filtering scatter plot between nCount_RNA and nFeature_RNA for the PBMC object.
- i) Total cell counts per PBMC sample following filtering.
- j) Doublets identified shown in the UMAP for PBMC object. These were removed from further analyses.

Fig. S2

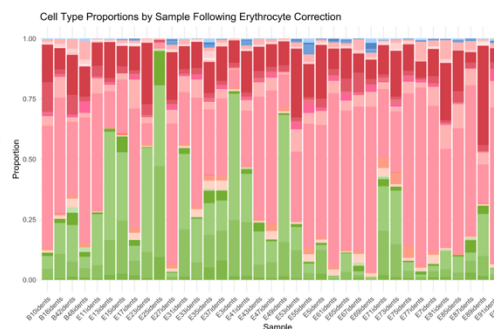
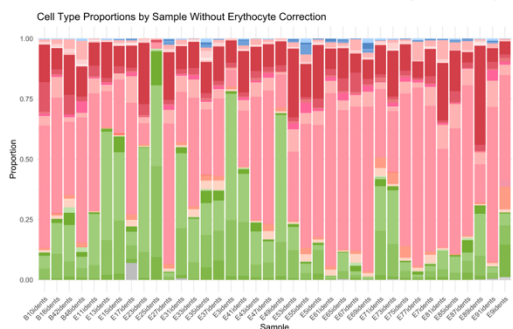
A



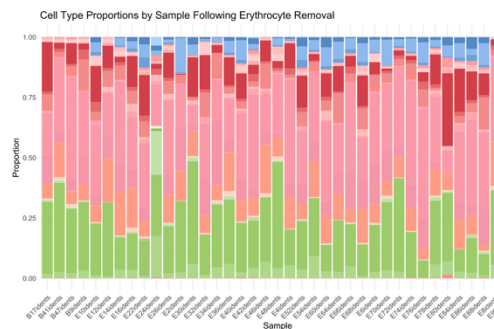
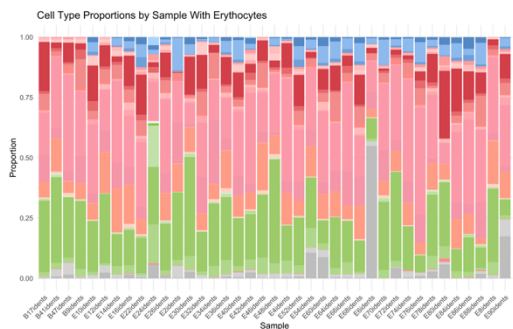
B



C All CSF cases before (left) and after (right) RBC/platelet removal



D All PBMC cases before (left) and after (right) RBC/platelet removal



E RBC/platelet removal for CSF cases from untreated and inactive MS vs HV comparison

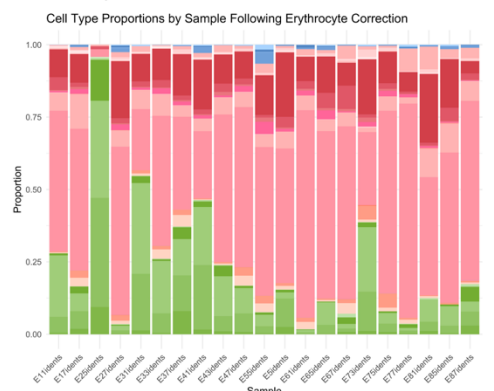
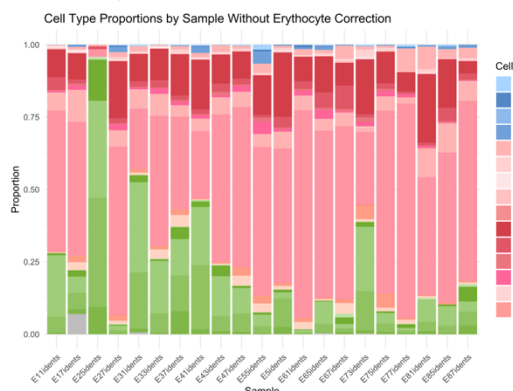
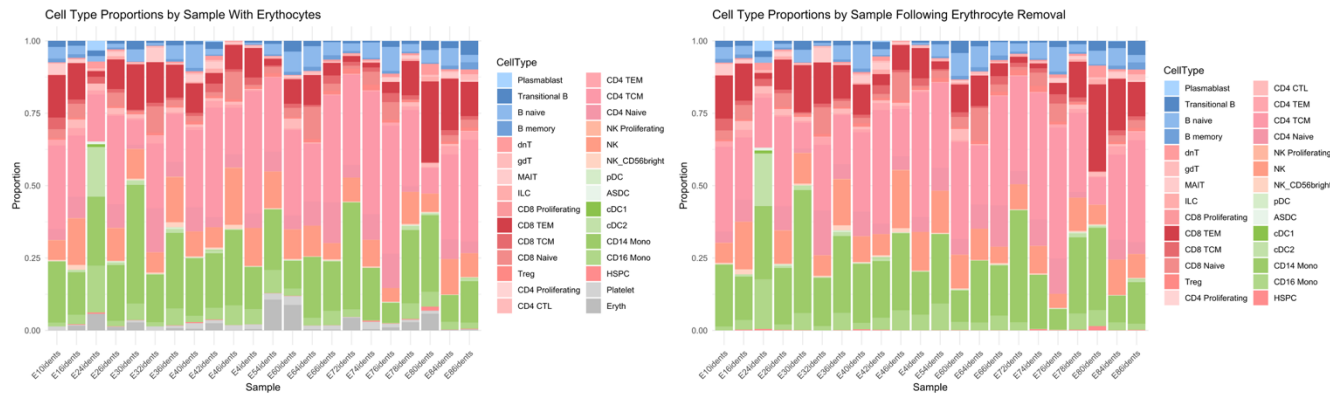
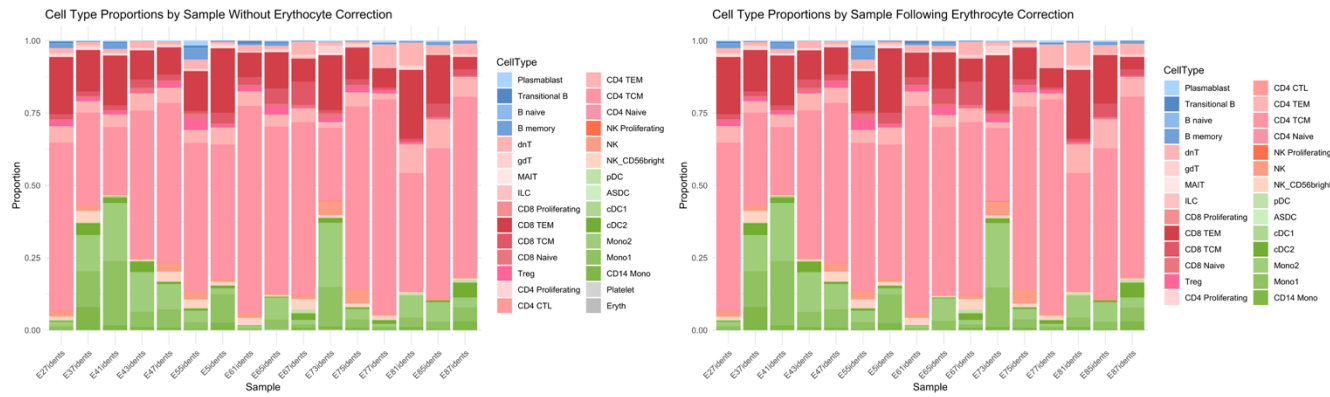


Fig. S2 continued

F RBC/platelet removal for PBMC cases from untreated and inactive MS vs HV comparison



G RBC/platelet removal for CSF cases from untreated and inactive PRL-positive vs PRL-negative comparison



H RBC/platelet removal for PBMC cases from untreated and inactive PRL-positive vs PRL-negative comparison

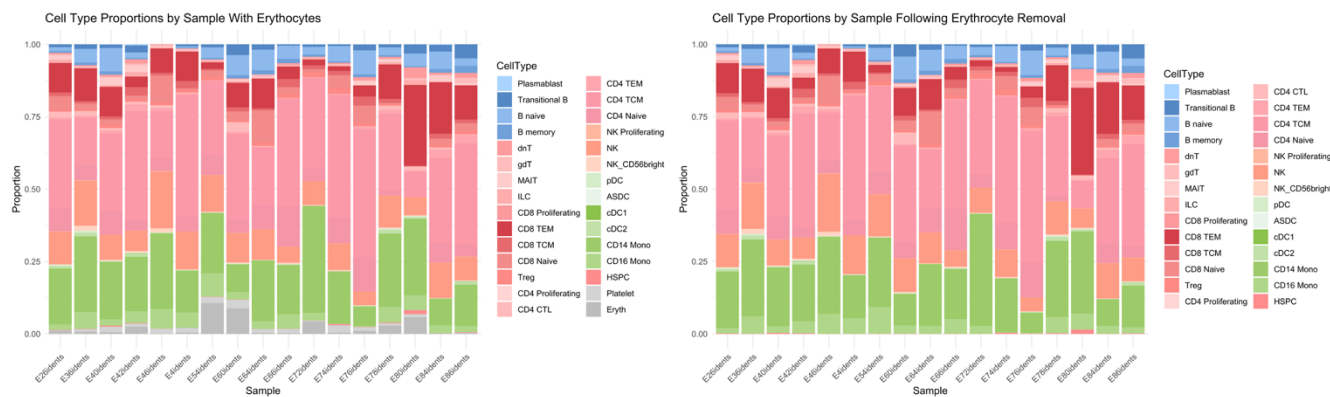


Figure S2: Erythrocyte and platelet removal (see Methods) does not impact cell proportions in the CSF and PBMC

- a) Overall CSF L1 UMAP representing cell populations, including erythrocytes and platelets.
- b) Overall PBMC L1 UMAP including erythrocytes and platelets.
- c) Stacked bar graph summarizing CSF L1 cell proportions prior to (left panel) and following (right panel) erythrocyte and platelet removal.
- d) Stacked bar graph summarizing PBMC L1 cell proportions prior to (left panel) and following (right panel) erythrocyte and platelet removal.
- e) CSF L1 cell proportions for the untreated and inactive MS vs. HV samples subsampled from the main CSF object, showing no to minimal change in proportions before and following erythrocyte and platelet removal.
- f) PBMC L1 cell proportions for the untreated and inactive MS vs. HV samples before and following erythrocyte and platelet removal, showing no to minimal change in proportions before and following erythrocyte and platelet corrections.
- g) Stacked bar graph showing CSF L1 cell proportions without and with erythrocyte and platelet removal for the PRL-positive vs. PRL-negative samples.
- h) Stacked bar graph showing PBMC L1 cell proportions without and with erythrocyte and platelet removal for the PRL-positive vs. PRL-negative samples.

Fig. S3

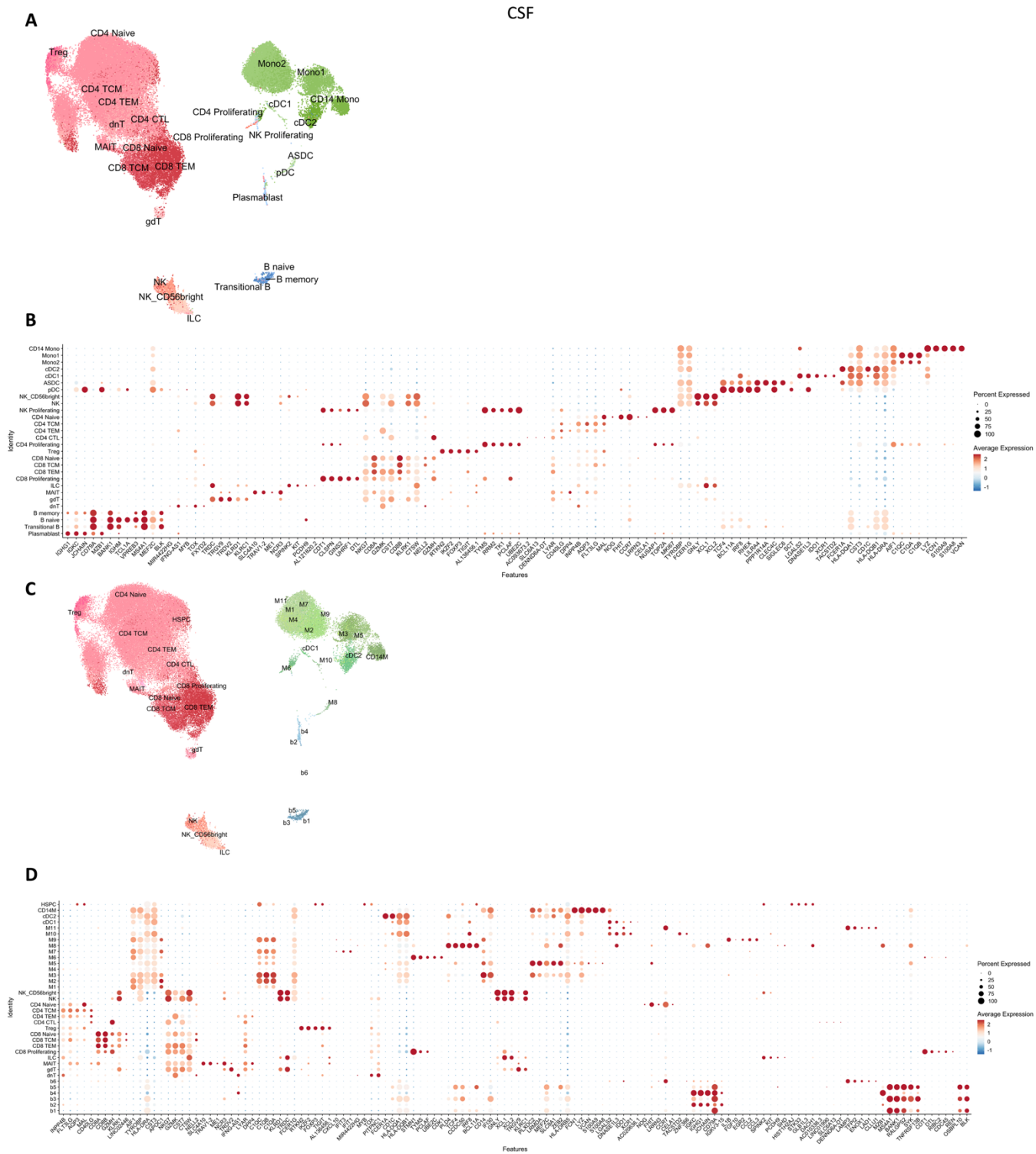


Fig. S3 continued

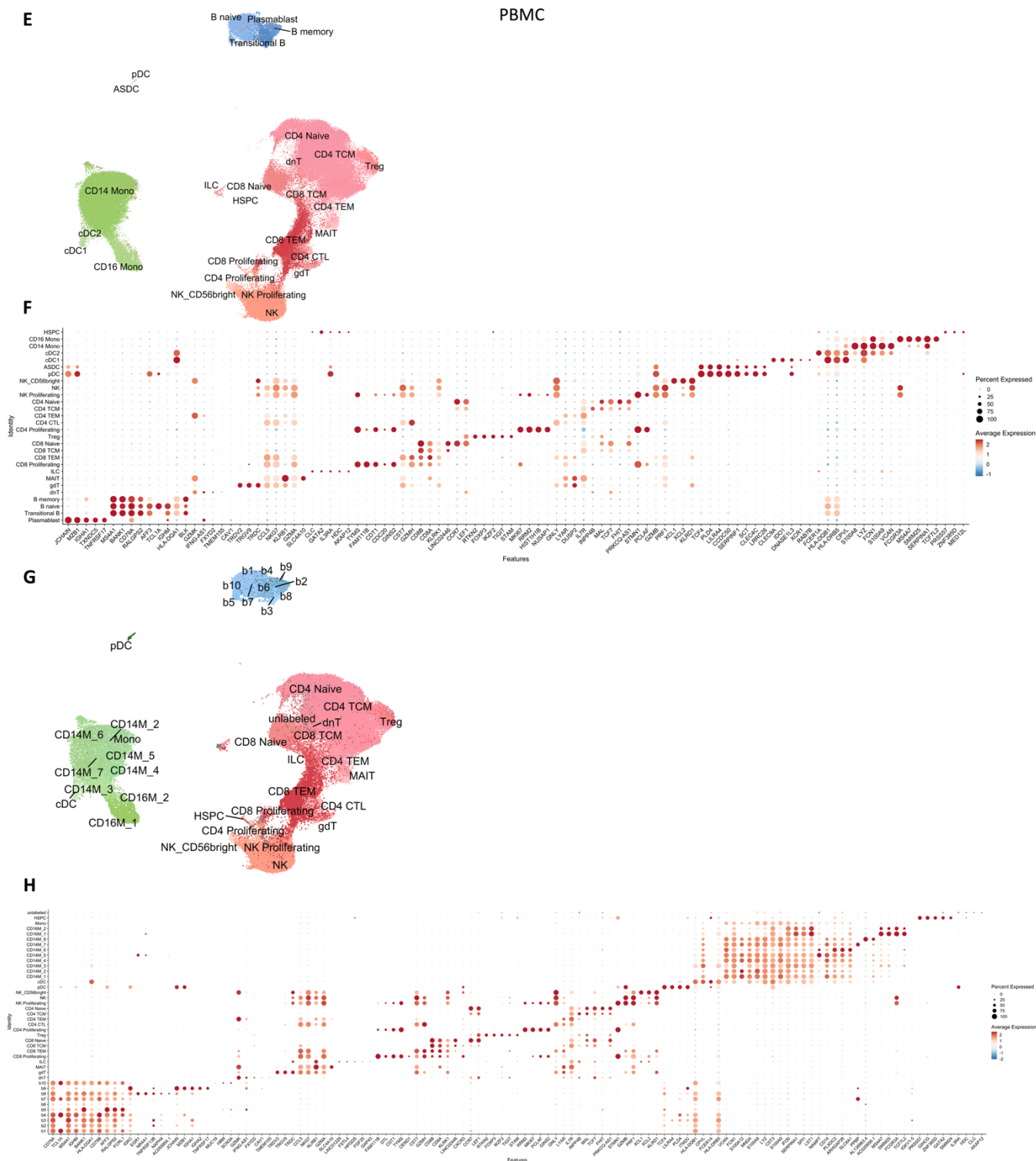


Figure S3: Top in-depth gene markers used for inferring cell populations in the CSF and PBMC

- a) CSF L1 UMAP with the cell populations shown.
- b) Dotplot representing top gene markers for the various L1 cell populations in the CSF.
- c) CSF UMAP with L2 cell annotations mapped onto L1 clusters.
- d) Dotplot summarizing the top gene markers for L2 annotated cell populations in the CSF.
- e) Scatterplot showing the L1 annotations for the PBMC.
- f) Dotplot representing the top gene markers for L1 cell annotated populations of the PBMC.
- g) PBMC UMAP with L2 cell annotations mapped onto L1 clusters.
- h) Dotplot summarizing the top gene markers for L2 annotated cell populations of the PBMC.

Fig. S4

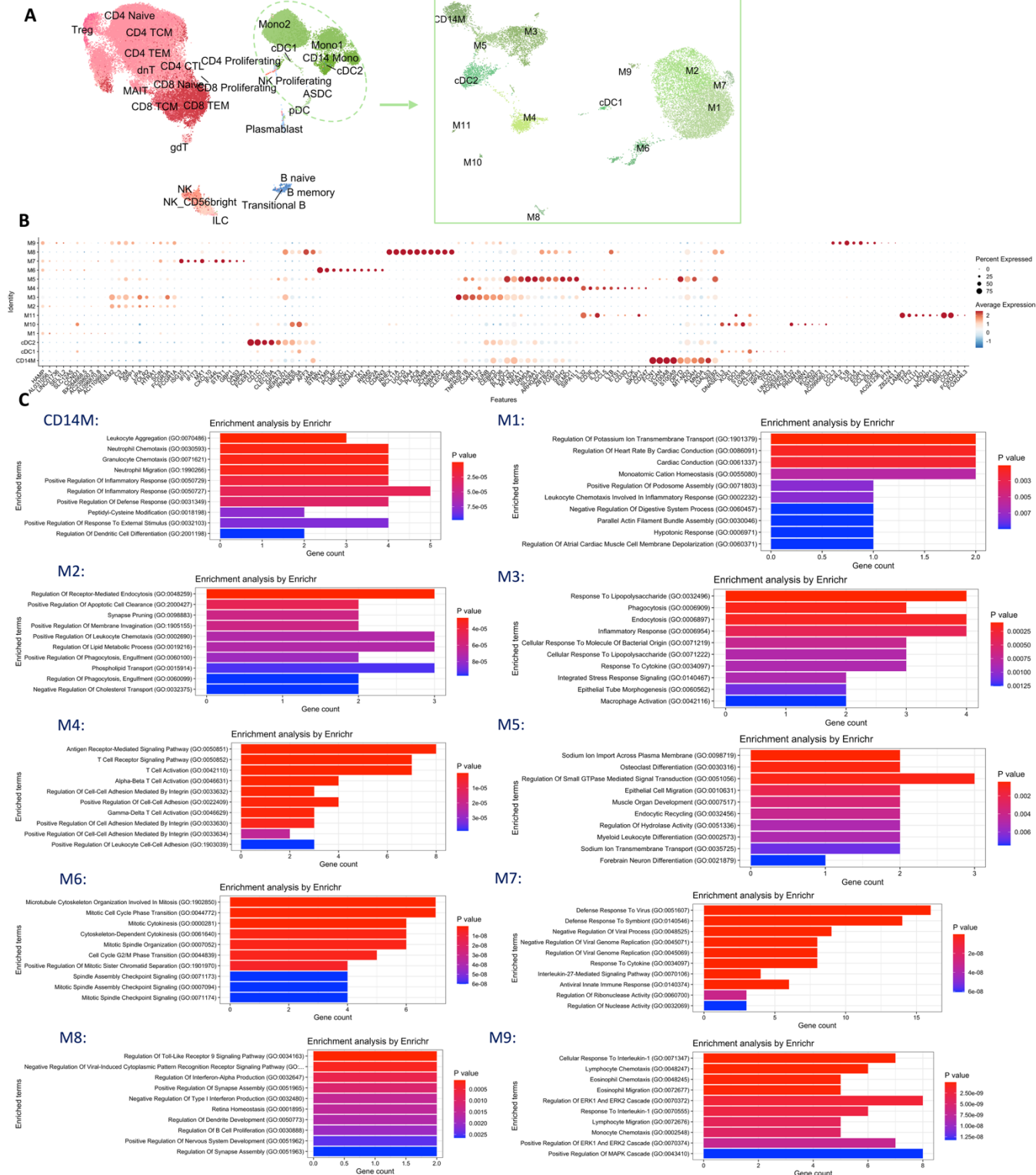
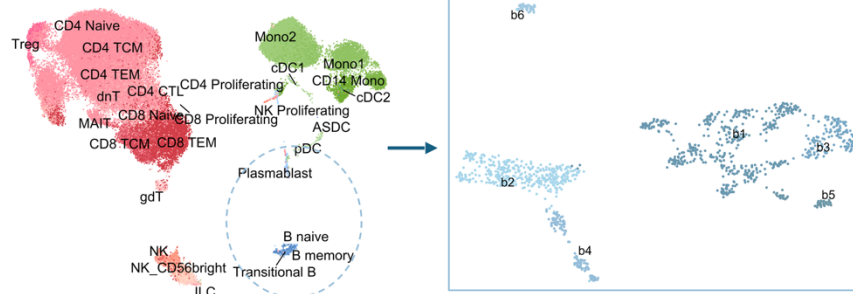


Figure S4: CSF myeloid subclusters demonstrate heterogeneity in function

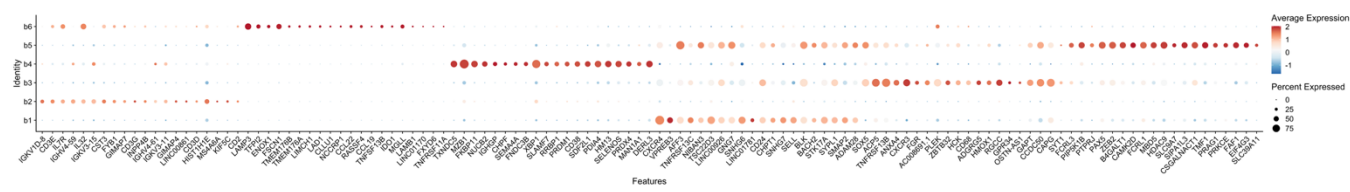
- a) CSF L1 UMAP showing the different populations, with the myeloid cells (encircled by a green dashed line) subclustered into L2 populations as shown in the right panel.
- b) Dotplot representing the gene markers of the myeloid subclusters. Average gene expression and the percentage of cells expressing the genes are shown.
- c) GO analyses of the top gene markers for the subclusters (see Methods to find how the top markers were found using FindMarker() function). GO terms, including majorly Biological Processes (BP) were used for annotating the marker gene lists. When required, additional subontologies including Molecular Function (MF), Cellular Component (CC), KEGG, Wiki, BioCarta, and Panther were used. CD14M subcluster was associated with leukocyte aggregation, neutrophil and granulocyte chemotaxis and positive regulation of inflammatory response. M1 enriched in regulation of potassium ion (K^+) transport, while M2 enriched in receptor-mediated endocytosis, synapse pruning, positive regulation of leukocyte chemotaxis and regulation of lipid metabolic process. M3 subcluster was associated with response to lipopolysaccharide (LPS), phagocytosis, endocytosis and inflammatory response. Gene markers identifying M4 subcluster enriched in antigen receptor-mediated signaling, while M5 showed association with sodium (Na^+) import, and regulation of small GTPase-mediated signaling. M6 was primarily associated with cell-cycle phases and mitotic spindle organization, while M7 was enriched for defense response to virus and regulation of viral genome replication. M8 enriched in Toll-like receptor (TLR) signaling, and M9 demonstrated enrichment for response to IL-1, ERK1/ERK2 cascade regulation, and chemotaxis of lymphocytes.

Fig. S5

A



B



C

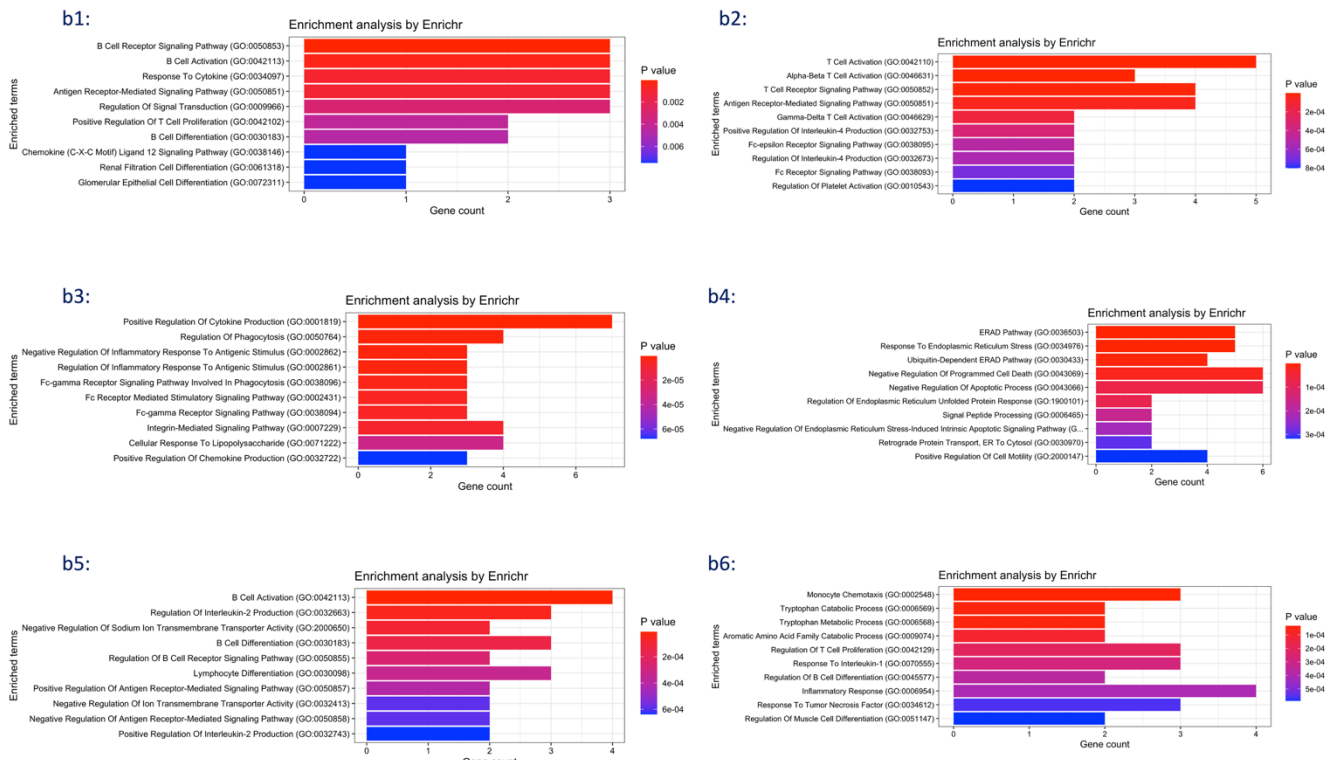
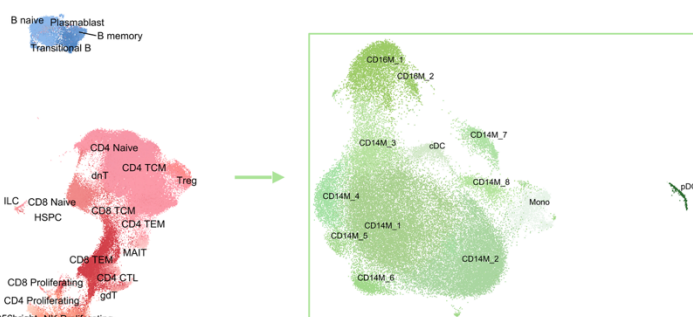


Figure S5: CSF B-lineage subclusters show transcriptional differences and varying functions

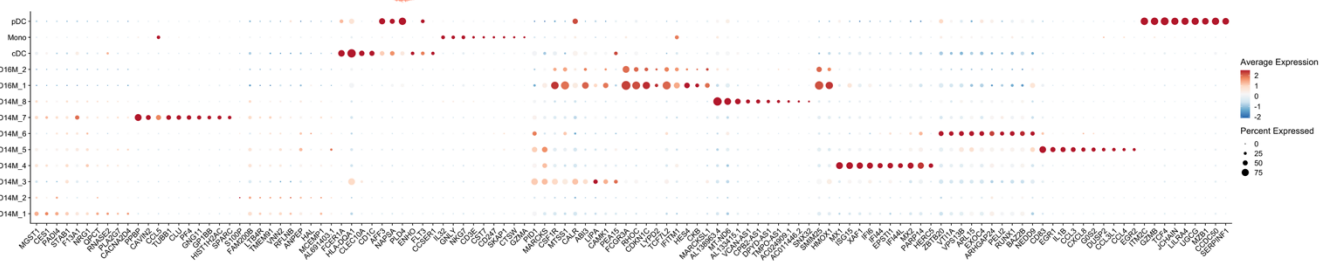
- a) CSF L1 UMAP and the B cell-lineage populations (encircled by a blue dashed line) subclustered into L2 populations as shown in the right panel.
- b) Dotplot showing the major gene markers for the subclusters.
- c) GO analyses of the subcluster defining genes. Predominantly, BP subontology was used to determine biological relevance. Subcluster b1 showed enrichment of B-cell receptor (BCR) signaling and B-cell activation, while b2 enriched for antigen-receptor mediated signaling and T-cell activation. Subcluster b3 enriched for cytokine production and regulation of phagocytosis. ERAD (Endoplasmic-Reticulum-associated protein degradation) pathway and response to ER stress were the terms associated with b4 cells, and B-cell activation and differentiation for b5 subcluster. Monocyte chemotaxis and tryptophan metabolism were the terms annotated for b6 population.

Fig. S6

A



B



C

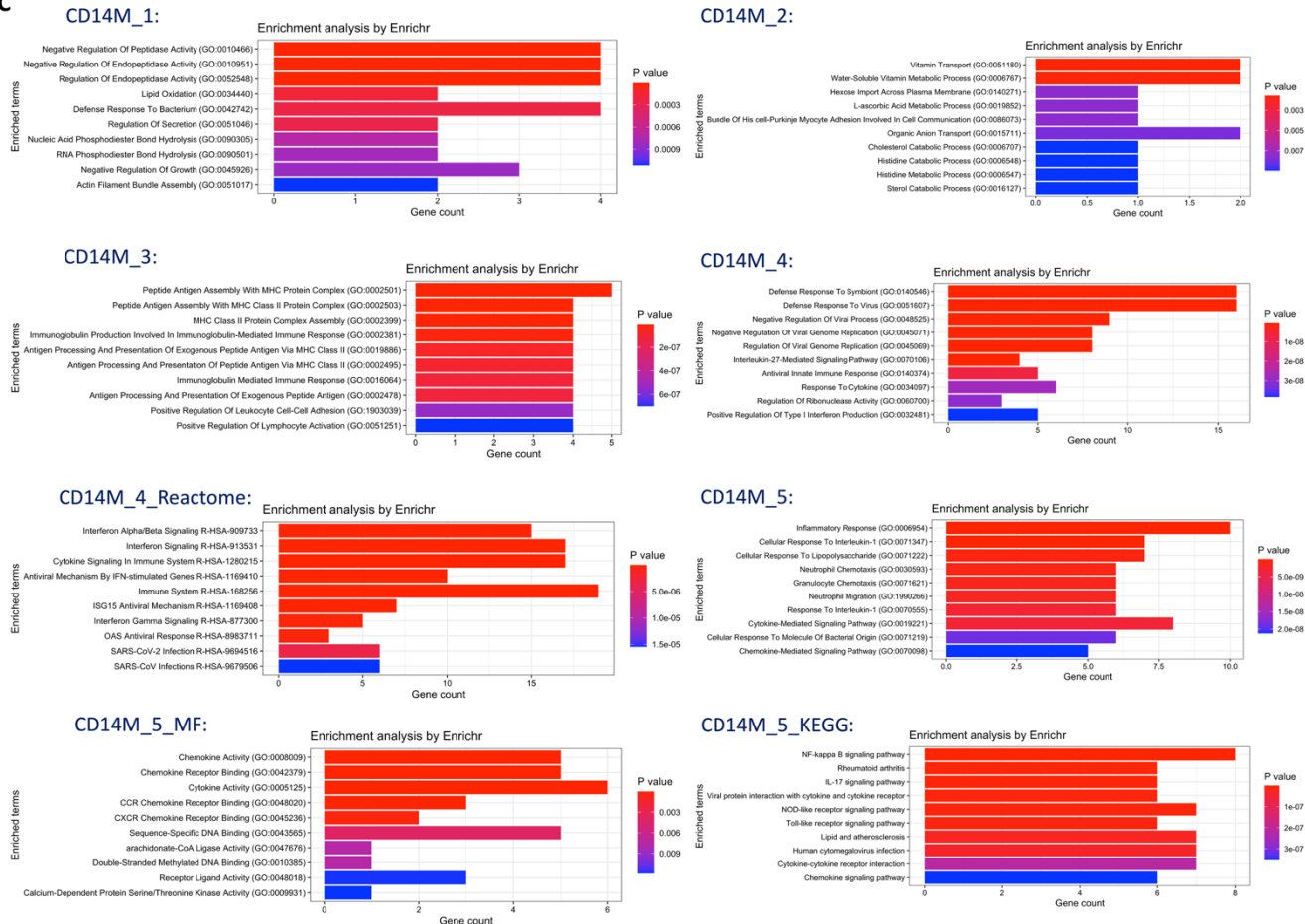


Fig. S6 continued

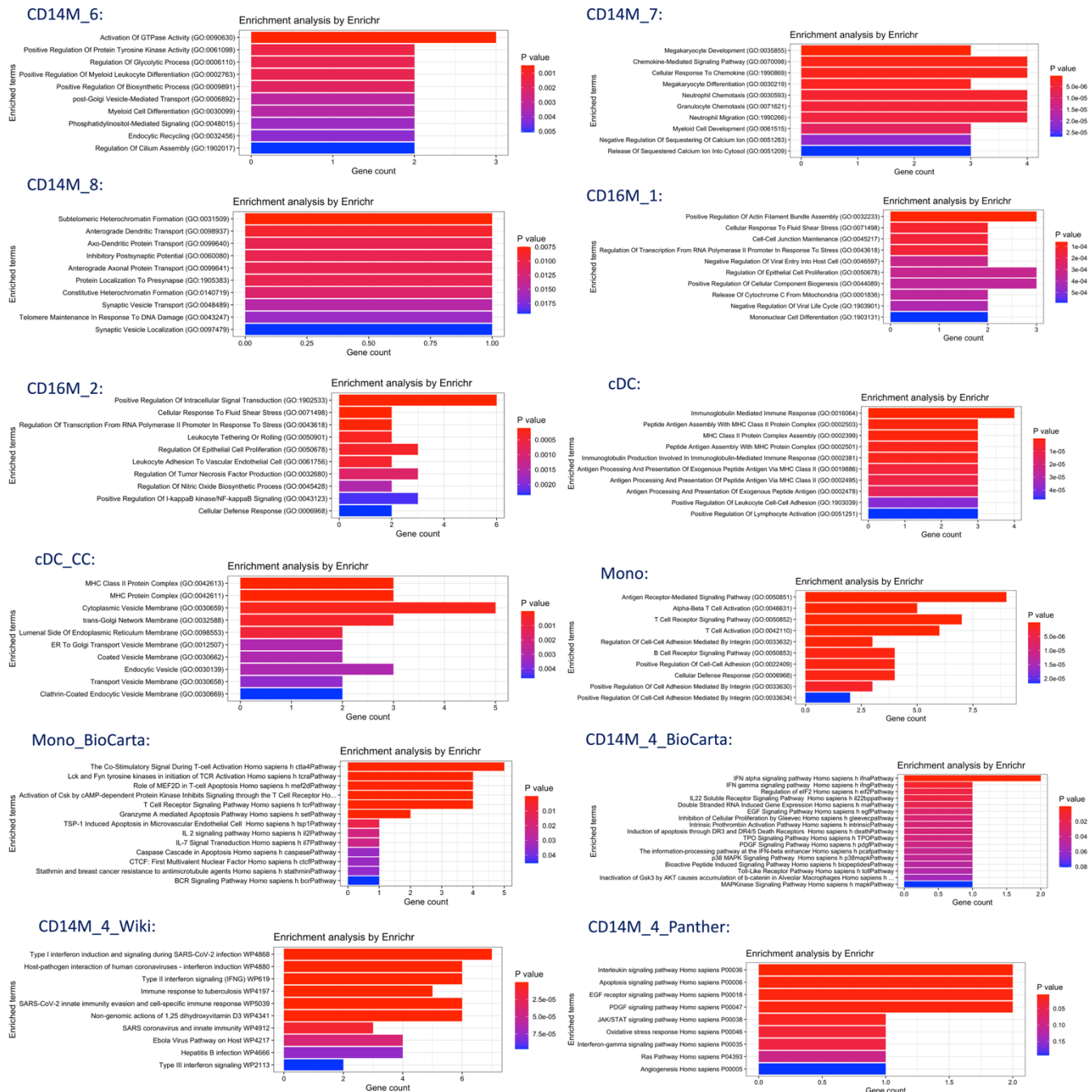
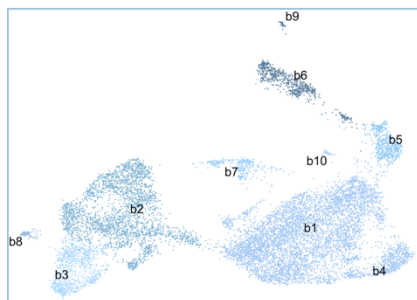
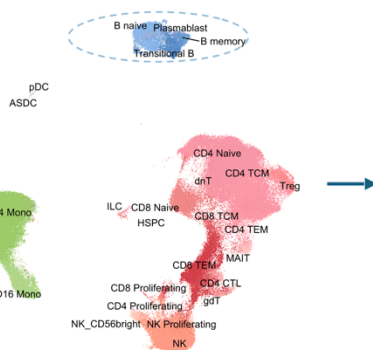


Figure S6: Peripheral myeloid cells subclusters and their ontologies

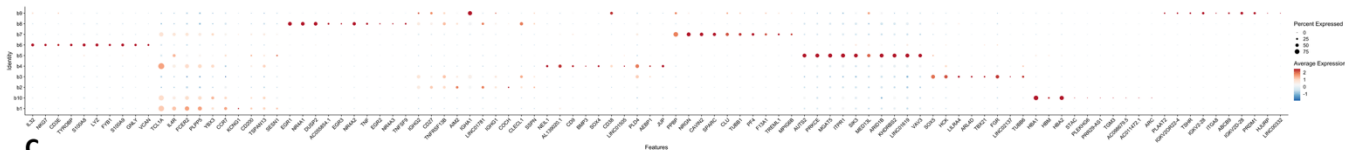
- a) PBMC L1 UMAP showing the myeloid cells and the subclusters in the right panel. The subclustering was performed on CD14 monocytes, CD16 monocytes, dendritic cells (cDC1, cDC2, ASDC, and pDCs).
- b) Dotplot illustrating the main cell markers for the peripheral myeloid subclusters.
- c) GO terms associated with CD14M_1 included negative regulation of peptidase activity and lipid oxidation. CD14M_2 monocytes enriched for vitamin-pertinent transport and metabolic processes. CD14M_3 monocytes had associations with peptide antigen assembly with MHC protein complex and MHC-II protein complex assembly. Notably, CD14M_4 monocytes enriched for terms including defense response to virus, antiviral immune response, positive regulation of type-I interferon production and type-II interferon signaling. Reactome subontology for CD14M_4 monocytes illustrate its role in interferon α/β (IFN- α/β) signaling, cytokine signaling, ISG15-antiviral mechanisms, and IFN- γ signaling. CD14M_5 monocytes enrich for inflammatory responses relevant to IL1 and LPS, and various chemotactic responses involving CXCR and CCR chemokine receptor binding. This subcluster is also enriched in NF- κ B, IL-17, NOD-like receptor and TLR signaling pathways. Note, additional subontologies mentioned above helped identify these annotations. CD14M_6 subcluster is enriched for activation of GTPase activity, positive regulation of protein tyrosine kinase and positive regulation of myeloid leukocyte differentiation. CD16M subclusters associated with cellular response to fluid shear stress and intracellular signal transduction. cDC, as expected, enrich in peptide antigen assembly with MHC-II protein complex, trans-Golgi network and ER-related processes.

Fig. S7

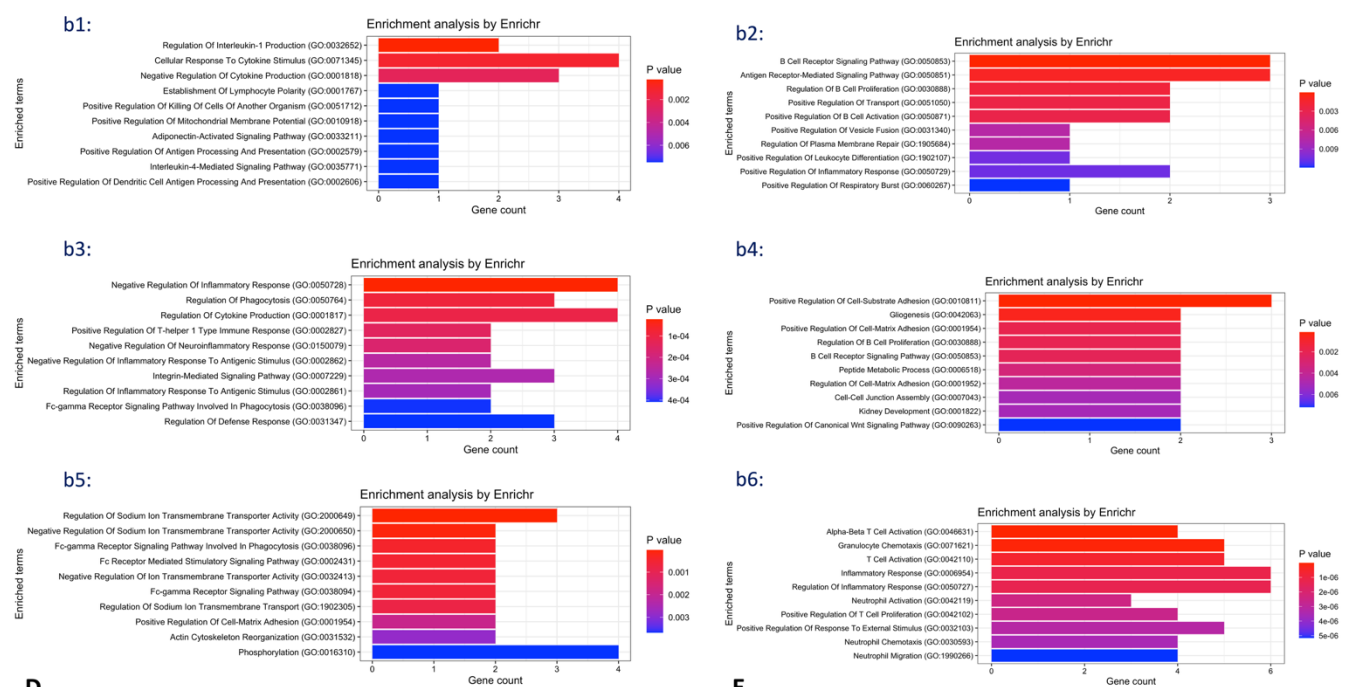
A



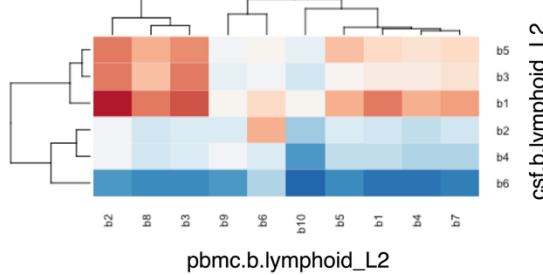
B



C



D



csf.b.lymphoid_L2

E

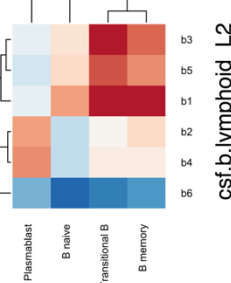
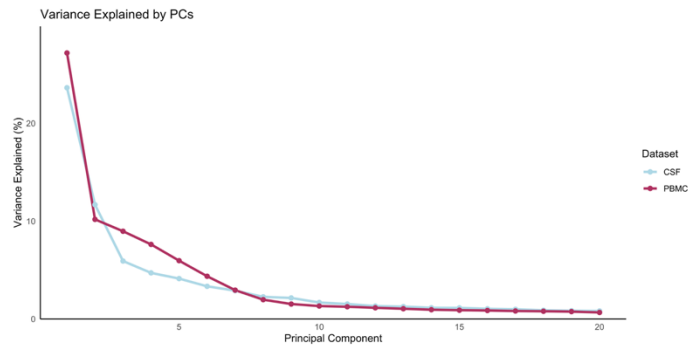


Figure S7: Peripheral B-cell subclusters and congruence with CSF B-lineage cells

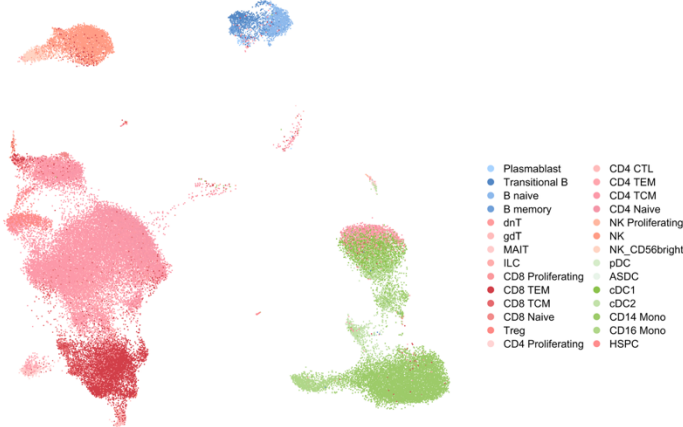
- a) PBMC L1 UMAP and representative B-cell populations with the subclusters shown in the right panel.
- b) Dotplot representing main markers for the subcluster populations of peripheral B-lineage cells.
- c) GO analyses of the individual peripheral B-lineage subclusters. The B-cell subcluster b1 enriched in regulation of IL-1 production and response to cytokine stimulus, b2 in B-cell receptor signaling, antigen-receptor mediated signaling and B-cell proliferation, b3 in negative regulation of inflammatory response and regulation of phagocytosis, b4 in positive regulation of cell-substrate adhesion, b5 in regulation of Na^+ ion transmembrane transporter activity and $\text{F}\gamma\text{c}$ -receptor mediated pathway involved in phagocytosis, and b6 in α/β T cell activation, granulocyte chemotaxis and T cell activation.
- d) Correlation heatmap showing transcriptional similarity between blood and CSF B-lineage clusters based on averaged transcriptional expression. Peripheral b6 B cell subcluster resembles the b2 subcluster in the CSF, which aligns with the matching ontologies of their respective gene markers.
- e) Correlation heatmap demonstrating transcriptional similarity between L2 CSF B-lymphoid clusters and main L1 CSF B-cell annotations.

Fig. S8

A



B



C

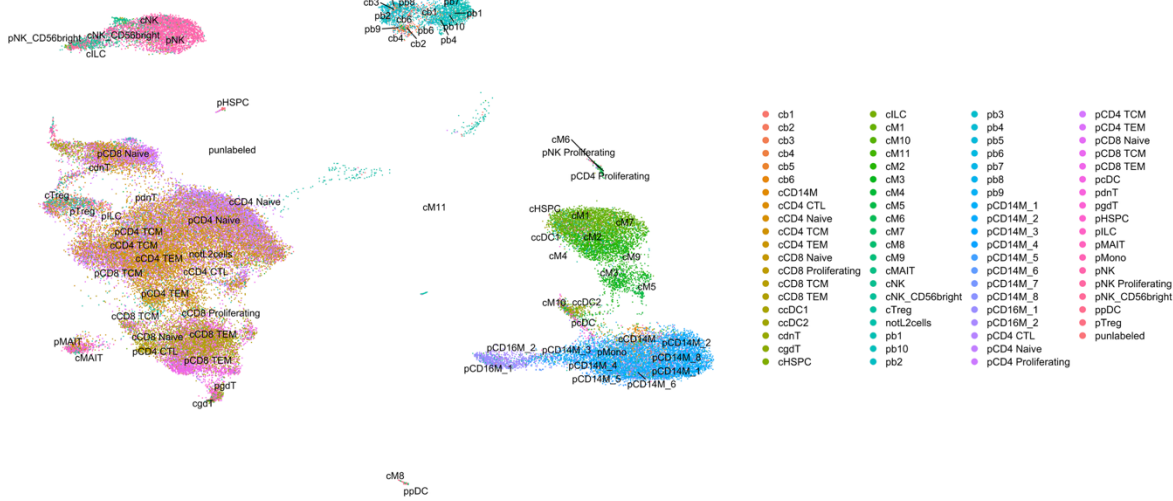
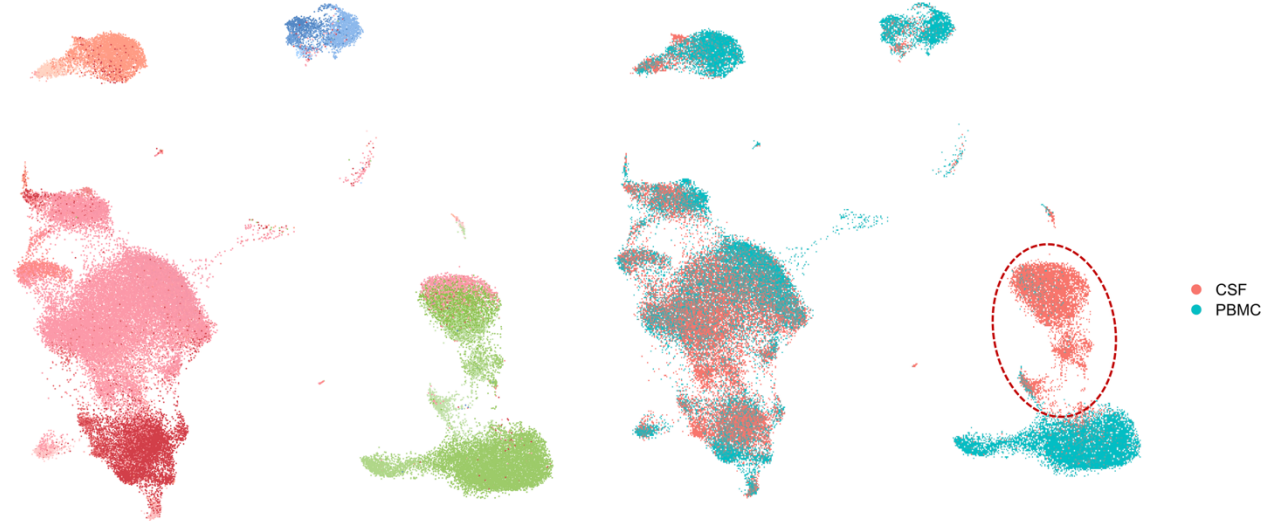
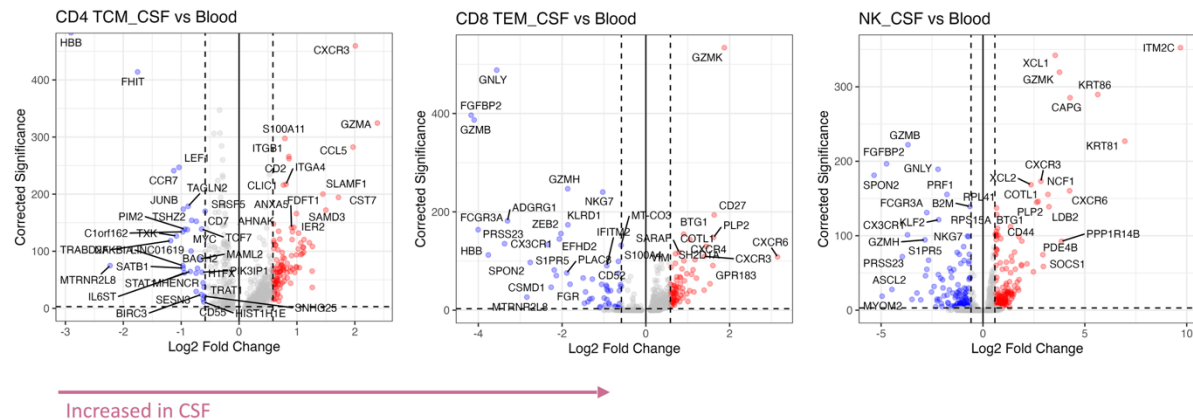


Fig. S8 continued

D



E



F

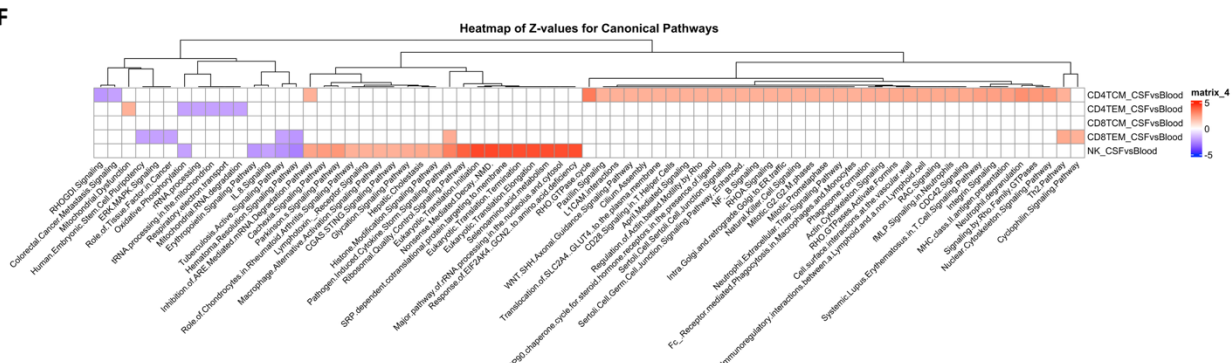
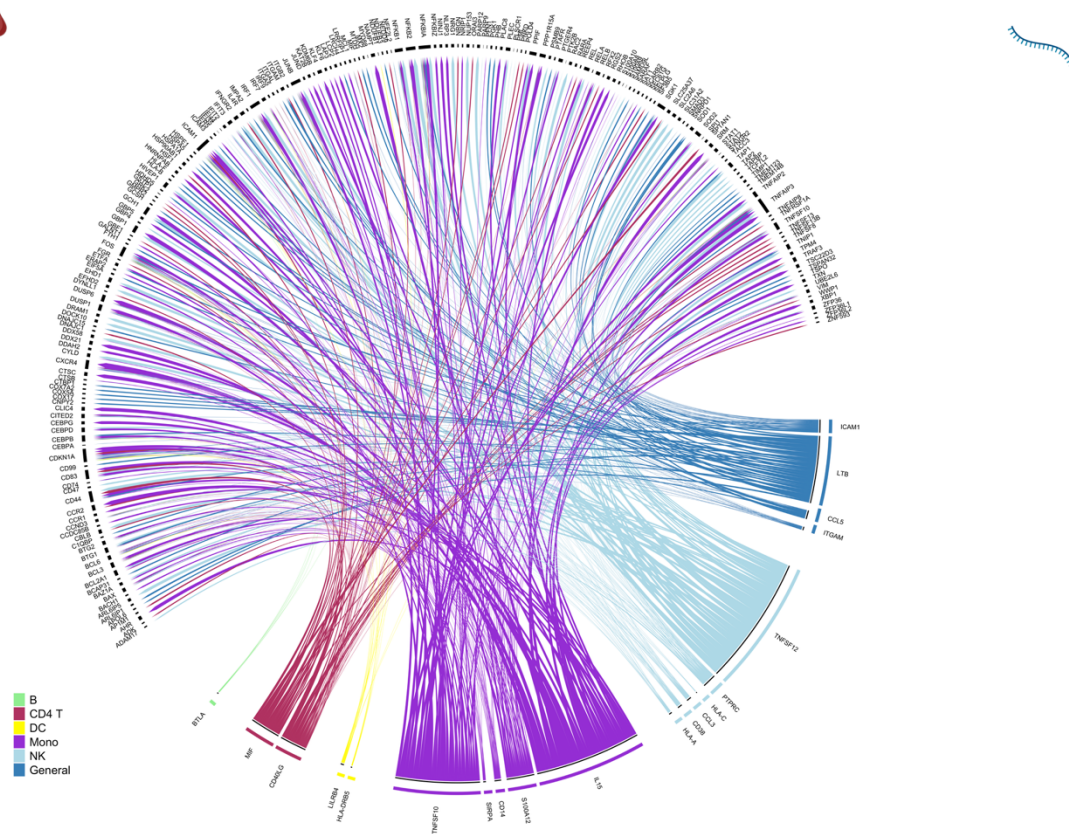


Figure S8: CD8 and CD4 T-cells upregulate genes associated with trafficking in CSF relative to blood

- a) Elbow plots for the variance explained by the PCs for CSF and PBMC objects.
- b) Combined UMAP (CSF cells and PBMC). Note that each sample was randomly down-sampled to 1000 cells before combination (if the sample had less than 1000 cells, the original number of cells were kept).
- c) Scatter plot illustrating L2 annotations from CSF cells and PBMC mapped back onto the combined UMAP object. The prefix 'p' represents cells from blood, while the prefix 'c' shows cells from the CSF.
- d) Scatter plot showing the immune-cell populations, and the separate clustering of CSF- and blood-derived myeloid cells.
- e) Volcano plots contrasting DEG across CSF relative to blood for the CD4-TCM, CD8-TEM, and NK cells from untreated and inactive PRL-positive and PRL-negative cases.
- f) Heatmap showing the Z-scores for pathway enrichment across the CSF versus blood comparison for T-lymphoid and NK cells.

Fig. S9

A



B

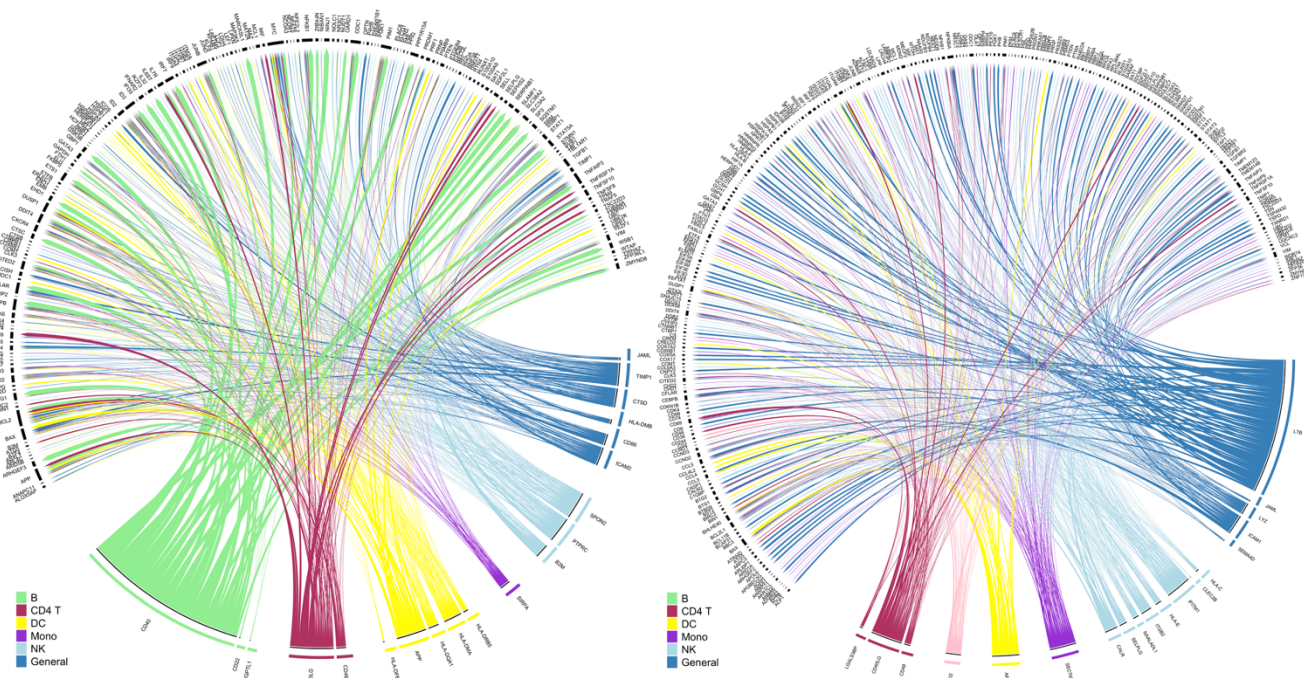


Fig. S9 continued

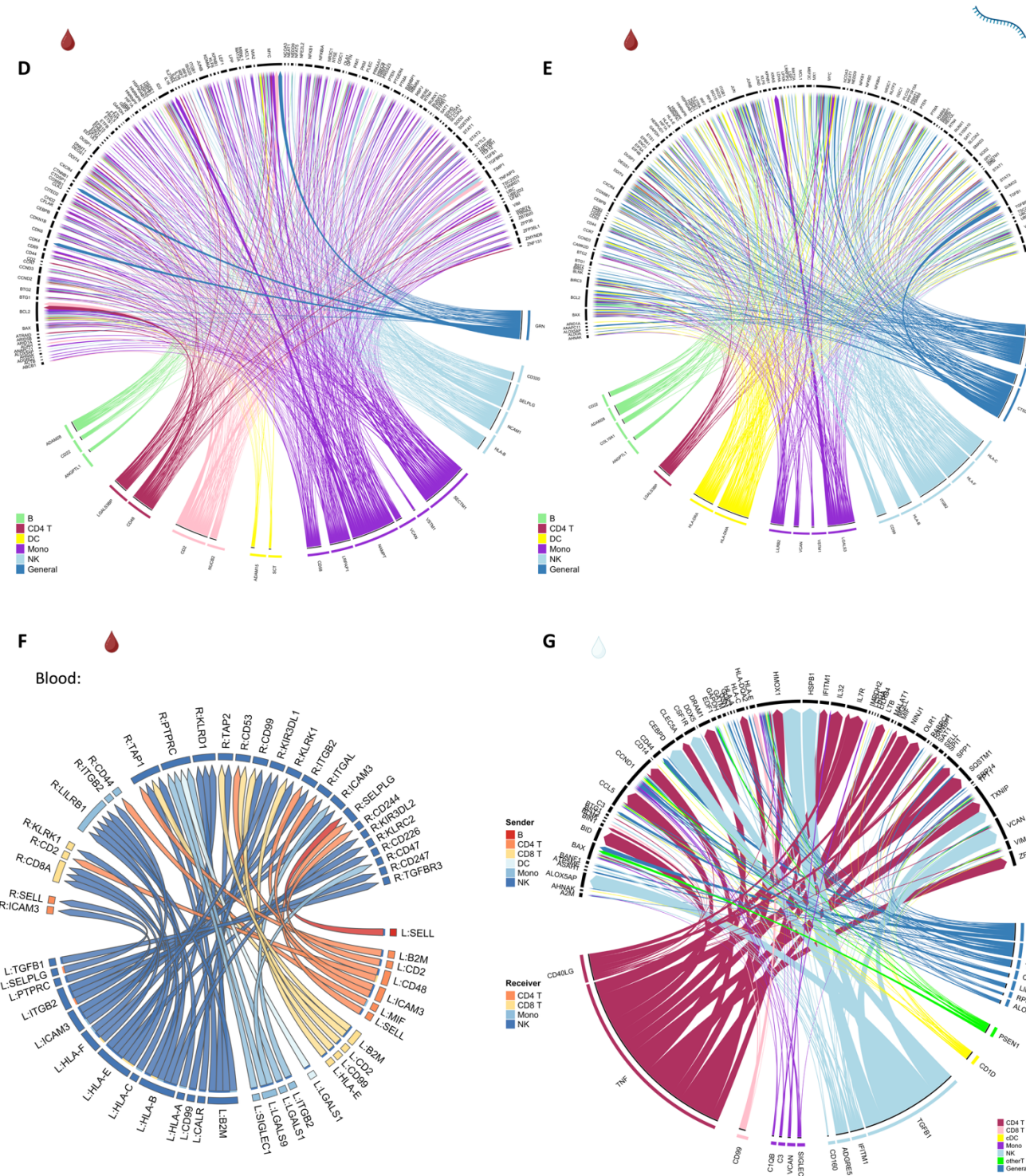


Figure S9: Interaction analyses between prioritized ligands (senders) and differentially expressed target genes across PRL-positive versus PRL-negative (receivers) reveal a myriad of ligands in regulating PRL-relevant pathology in the blood

Circos plots summarizing the interactions between prioritized ligands and target genes of myeloid (a), CD4-T (b), NK (c), CD8-T (d), and B (e) cells for PRL-positive versus PRL-negative in the blood. Note the different prioritized ligands for each receiving cell type. These include *HLA-E*, *HLA-C*, *IFITM1*, *LTB*, and *CD40LG* for NK cells; *CD48*, *LRPAP1*, and *SECTM1* for CD8 T-cells; *CD40*, *CD48*, *APP*, *PTPRC*, and *TIMP1* for CD4 T-cells, and *HLA-DRA*, *LGALS3*, *ITGB2*, *CTSD*, and *TGFB1* for B-cells.

Prioritized LR-network for peripheral immune cells (f) representing differentially abundant interactions with senders being primarily NK cells and receivers including CD8-T, CD4-T, Mono and NK cells. Note, the MHC-I related genes act as ligands in the peripheral network with receptors including *CD8A*, *KLRK1*, *KLRKC*, and *LILRB1* to name a few.

Fig. S10

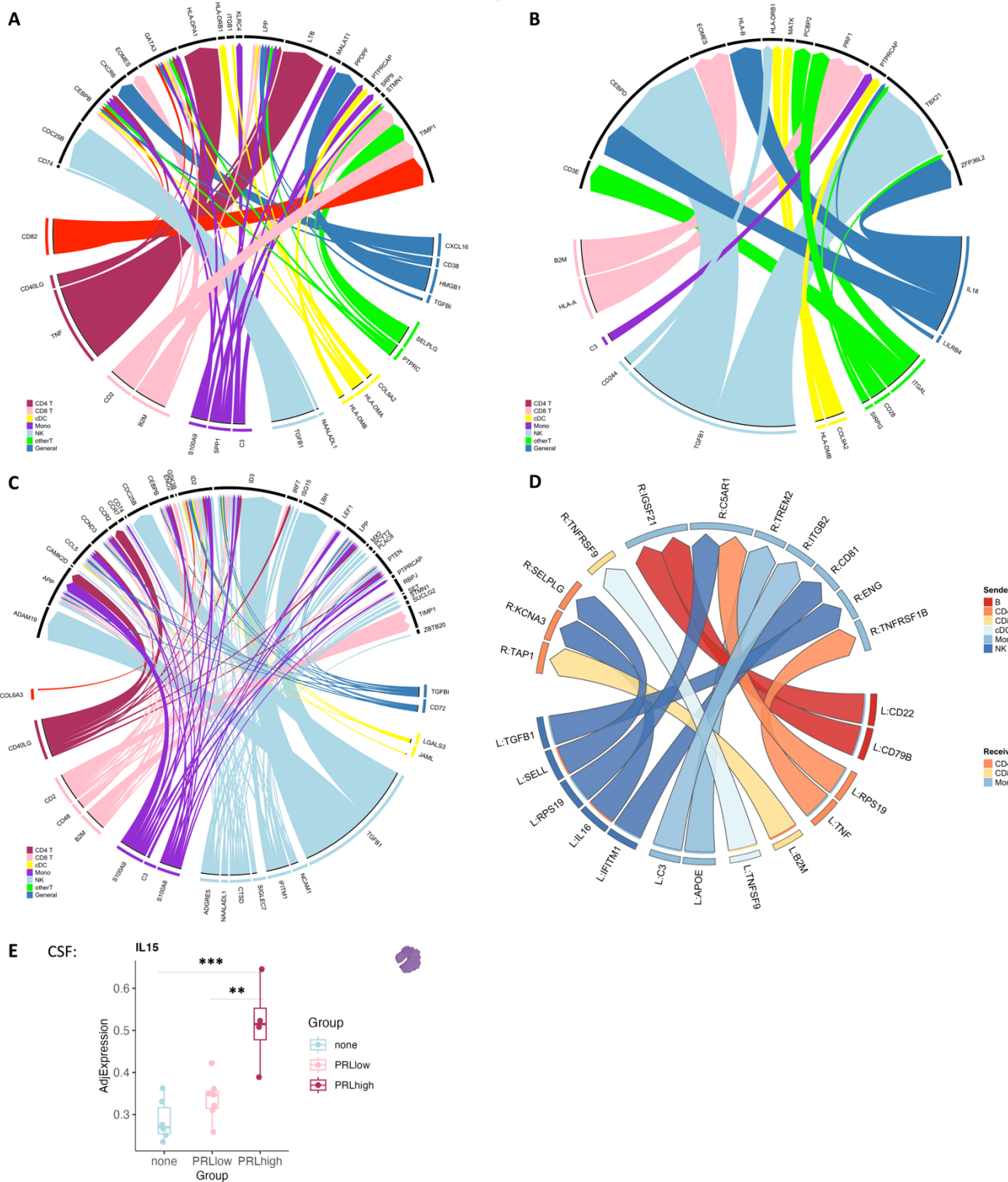


Figure S10: Interaction analyses between prioritized ligands (senders) and differentially expressed genes across PRL-positive versus PRL-negative as the target genes in the CSF cells reveal the regulatory roles of TNF, TGFB1, and CD47 among many molecules. Regulatory potential of IL15.

Circos plots summarize the interaction analyses between the prioritized ligands and target genes for myeloid cells (Figure S9G), CD8-T (a), NK (b), and CD4-T cells (c) for PRL-positive vs. PRL-negative in the CSF. These include *TNF*, *TGFB1*, and *CD40LG* for myeloid cells (labeled as Mono for these analyses – see **Methods**). For CD8 T-cells, the prioritized ligands regulating the PRL-positive state included *TNF*, *TGFB1*, *CXCL16*, *SPP1*, and *C3*, and for CD4 T-cells, the prioritized ligands included *TGFB1*, *IFITM1* and *SIGLEC7*. *TGFB1*, *CD244*, *C3*, *ITGAL*, and *IL18* were the prioritized ligands for NK-cells.

Prioritized LR-network for the CSF (d) demonstrating differentially abundant interactions contributing to PRL pathology. There is relative predominance of myeloid (Mono) cells as the receivers in the prioritized networks for CSF. Significant interactions involving myeloid activation include *C3*, *APOE*, *IFITM1*, *TNF*, *TGFB1*, and *RPS19* as ligands for receptors mostly present on myeloid cells. Notable also are the CD4 T-cells acting as receivers, while B, NK and CD8 T-cells act as the senders. The annotations used for the NicheNet analyses are the simplest level annotations to improve the significance and strength of intercellular communication level analyses.

IL15 abundance in the CSF across patients from different PRL-categories (e) (**p< 0.005, ***p < 0.001).